

PRICES SUBJECT TO CHANGE

**FINAL REPORT**

Reproduced by  
**NATIONAL TECHNICAL  
INFORMATION SERVICE**  
US Department of Commerce  
Springfield, VA. 22151

**DEVELOPMENT OF A GAS PRESSURE BONDED  
FOUR-POLE ALTERNATOR ROTOR**

BY

**G. G. LESSMANN AND W. A. BRYANT**

PREPARED FOR

**NATIONAL AERONAUTICS AND SPACE ADMINISTRATION**

**CONTRACT NAS 3-11837**

**NASA LEWIS RESEARCH CENTER**

**CLEVELAND, OHIO 44135**

**J. A. MILKO, PROJECT MANAGER**



**Astronuclear Laboratory**

**Westinghouse Electric Corporation**

(NASA-CR-120923) DEVELOPMENT OF A GAS  
PRESSURE BONDED FOUR-POLE ALTERNATOR ROTOR  
Final Report (Westinghouse Astronuclear  
Lab., Pittsburgh)

G3/09

N74-30574

Unclas  
46214

## NOTICE

This report was prepared as an account of Government-sponsored work. Neither the United States, nor the National Aeronautics and Space Administration (NASA), nor any person acting on behalf of NASA:

- A.) Makes any warranty or representation, expressed or implied, with respect to the accuracy, completeness, or usefulness of the information contained in this report, or that the use of any information, apparatus, method, or process disclosed in this report may not infringe privately-owned rights; or
- B.) Assumes any liabilities with respect to the use of, or for damages resulting from the use of, any information, apparatus, method or process disclosed in this report.

As used above, "person acting on behalf of NASA" includes any employee or contractor of NASA, or employee of such contractor, to the extent that such employee or contractor of NASA or employee of such contractor prepares, disseminates, or provides access to any information pursuant to his employment or contract with NASA, or his employment with such contractor.

*id*

## DEVELOPMENT OF A GAS PRESSURE BONDED FOUR-POLE ALTERNATOR ROTOR

by

G. G. Lessmann  
and  
W. A. Bryant

Westinghouse Astronuclear Laboratory

April, 1972

Prepared for

National Aeronautics and Space Administration  
NASA-Lewis Research Center

Contract NAS 3-11837

J. A. Milko, Project Manager

## ABSTRACT

Methods were developed for fabrication of a solid four pole alternator rotor by hot isostatic pressure welding. The rotor blanks welded in this program had complex geometrical mating interfaces and were of considerable bulk, being approximately 3-1/2 inches (0.089 meters) in diameter and 14 inches (0.356 meters) long. Magnetic end pieces were machined from AISI 4340 steel, while the non-magnetic central section was of Inconel 718. Excellent welds were produced which were shown to be responsive to post weld heat treatments which substantially improved joint strength. Prior to welding the rotors, test specimens of complex geometry were welded to demonstrate that complex surfaces with intentional mechanical misfit could be readily joined using HIP welding. This preliminary work demonstrated not only that interface compliance is achieved during welding but that welding pressure is developed in these thick sections sufficient to produce sound joints. Integral weld-heat treatment cycles were developed that permitted the attainment of magnetic properties while minimizing residual stress associated with the allotropic transformation of 4340 steel.

## FOREWORD

This report describes the work performed under Contract NAS 3-11837 during the period December 1968 to December 1970. The experimental program was administered under the Space Power Systems Division of the National Aeronautics and Space Administration with Mr. J. A. Milko acting as project manager.

This work was administered at the Astronuclear Laboratory by Mr. R. W. Buckman with Mr. G. G. Lessmann serving as principal investigator.

## TABLE OF CONTENTS

<u>Section</u>	<u>Title</u>	<u>Page</u>
	ABSTRACT	
I.	SUMMARY	1
II.	INTRODUCTION	2
III.	EXPERIMENTAL PROCEDURES	11
IV.	RESULTS AND DISCUSSION	30
	A. Rotor Welding	30
	B. Outgassing of 4340	34
	C. Surface Preparation	38
	D. Weld Temperature	42
	E. Weld Hold Time	43
	F. Weld Pressure	43
	G. Heat Treatment	45
	H. Magnetic Permeability	45
	J. Alternate Magnetic Materials	47
V.	CONCLUSION	53
VI.	REFERENCES	54
	APPENDIX A – Data Summary Sheets for Preliminary Welding Trials	

## LIST OF TABLES

<u>Table No.</u>	<u>Title</u>	<u>Page</u>
1	Fracture Strength Results Obtained from Rotor Verification Specimens	32
2	Comparison of Tensile Strengths of Welds Prepared with Specimens Containing Outgassed and Non-outgassed 4340 Steel	35
3	Joint Strengths of Welds Employing Vacuum Melted Steel Compared to Ones for Non-Vacuum Melted Steel	39
4	Tensile Strengths of Welds Prepared with Various Surface Preparations	41
5	Weld Tensile Strength Data for Two Hold Times	44
6	Effect of Post Weld Heat Treatment and Joint Orientation on Joint Strength	46
7	Magnetic Permeability of 4340 Steel Associated with a Number of Integral Heat Treatments	49
8	Weld Tensile Strengths of Hyperco 50 - Inconel 718 Couples	50

## LIST OF FIGURES

<u>Figure No.</u>	<u>Title</u>	<u>Page</u>
1	Outline Drawing of Finished Rotor	3
2	Schematic Drawing of Brayton Cycle Turbo Alternator-Compressor Unit	4
3	Dilatometer Measurement Data for Inconel 718 and AISI 4340	7
4	Rotor Blank Components Prior to HIP Welding	12
5	Simple Weld Specimen	13
6	Complex Weld Specimens	14
7	Type I Mismatch Specimen	15
8	Type II Mismatch Specimens	16
9	End Cap for Can Used in HIP Welding	18
10	Rowland Ring Specimen	19
11	Photograph of Portion of Specimens Used in Experimental Program	20
12	Geometric Orientation of Bend Coupons Machined from Simple, Flat-Faced Specimen. Transverse Section Through Welded Specimen is Portrayed	24
13	Sketch Showing Location of Tensile and Metallographic Specimen Blanks Within Welded Type II Mismatch Specimen	25
14	Weld Joint Tensile Specimen	26
15	Sketch Showing Location of Tensile and Metallographic Specimen Blanks Within Welded Type I Mismatch Specimen	27
16	Sections A-A and B-B of Figure 15	28
17	HIP Welded Rotor Blank. Canning Material has been Machined off Central Section	31
18	Weld Interface of Verification Specimen HIP Welded With Rotor Blank	33
19	Photomicrographs of HIP Welded 4340/718 Joints. Note the Complete Absence of the Thinner Diffusion Region that is Usually Associated with Weld Joint Failure	36



## LIST OF FIGURES (Continued)

<u>Figure No.</u>	<u>Title</u>	<u>Page</u>
20	Results of Microhardness Traverses of Weld Specimen Inter-diffusion Zones	37
21	Comparison of Modes of Failure in Tensile Specimens Tested from HIP Welds	40
22	Magnetization Curves for Material from Two Welding Trials Compared to that for a Control Sample	48
23	Microstructure of Inconel 718 - Hyperco 50 Weld Specimen. Hyperco 50 was Etched Prior to Welding	51
24	Microstructure of Inconel 718 - Hyperco 50 Weld Specimen. Hyperco 50 was not Etched Prior to Welding	52

## I. SUMMARY

Two solid four pole alternator rotors were fabricated by hot isostatic pressure (HIP) welding. The rotor blanks, which had complex geometrical mating interfaces, were 3-1/2 inches (0.089 m) in diameter and 14 inches (0.356 m) long. Magnetic end pieces were machined from AISI 4340 steel, while the non-magnetic central section was Inconel 718. After outgassing the AISI 4340 end pieces at 1800°F (982°C) for 24 hours (86.5 ks) and  $10^{-5}$  torr ( $1.332 \text{ mN/m}^2$ ), they were assembled to the cleaned Inconel 718 central section. The assembly was clad with type 304 stainless steel sheet, evacuated and sealed by electron beam welding. HIP welding of the assembly was accomplished by heating for 4 hours (14.4 ks) at 1750°F (954°C) under a pressure of 29,000 psi ( $200 \text{ MN/m}^2$ ). The assembly was then cooled while maintaining pressure to 1200°F (650°C) where it was held for 8 hours (28.8 Ms) in order to achieve the desired magnetic properties. Bend fracture strengths of 119,700 - 128,500 psi ( $825 - 885 \text{ MN/m}^2$ ) were obtained on control specimens bonded with the rotors. Hardness test results indicated that greater than 96% of the desired magnetic permeability (18.0 kilogauss (1.80 T) with a magnetizing force of 100 oresteds (7.960 mA/m) was achieved in the 4340.

Prior to welding the rotors, a series of HIP welding runs were made to ascertain the effects of surface preparation, time at temperature, temperature, and interface fit-up on the properties of the 4340/Inconel 718 joint. Vacuum outgassing pretreatment of the 4340 was shown to be critical to achieve consistently sound joints with the Inconel 718 during bonding at 1750°F (954°C) and 29,000 psi ( $200 \text{ MN/m}^2$ ). Heat treatment integral with the HIP welding cycle developed optimum magnetic properties while minimizing the residual stress associated with the allotropic transformation of the 4340. The tensile strength of the 4340/Inconel 718 joint optimum magnetic condition was 82,500 psi ( $569 \text{ MN/m}^2$ ). Joint strengths however were increased to as high as 141,800 psi ( $975 \text{ MN/m}^2$ ) by post bond heat treatments. The higher joint strengths were achieved, however, at the expense of magnetic properties.

## II. INTRODUCTION

Techniques were developed for fabricating two alternator rotor blanks by hot isostatic pressure welding (HIP Welding\*). In this process a weldment is produced by canning the assembly in an evacuated and sealed container which is then subjected to an external isostatic pressure and elevated temperature. Welding results from the intimate contact between parts achieved when the combination of pressure and temperature is sufficient to overcome mechanical and chemical surface barriers.

An outline drawing of the finished rotor is shown in Figure 1. This rotor is designed for use in a turboalternator-compressor unit for a Brayton cycle conversion system and is shown schematically in Figure 2. Its nominal operation at 36,000 RPM provides an output of 6 kw at 1200 cycles per second (1200 Hz). The rotor is of the Lundell type and is fabricated into a solid four pole configuration using double pole end pieces of AISI 4340 steel bonded to a complex central section of cast Inconel 718.

Before proceeding with a description of the program instituted for welding the rotors, it would be advantageous to first review the basic aspects of the HIP welding process in order to establish the underlying principles or guidelines for the program.

The formation of a weld between two solid bodies by means of HIP welding is accomplished by bringing the surfaces to be joined into intimate contact sufficient to permit metallurgical bonding between the mating surfaces. For ideal surfaces (those which are perfectly flat and atomically clean) this intimate contact is readily achieved. However, in order to achieve intimate contact between two non-ideal surfaces, several barriers must first be overcome.

---

\* This terminology has been suggested by Moore and Holko<sup>(1)</sup> and will be used throughout this report (instead of gas pressure bonding) to define the solid state welding process used in this program.

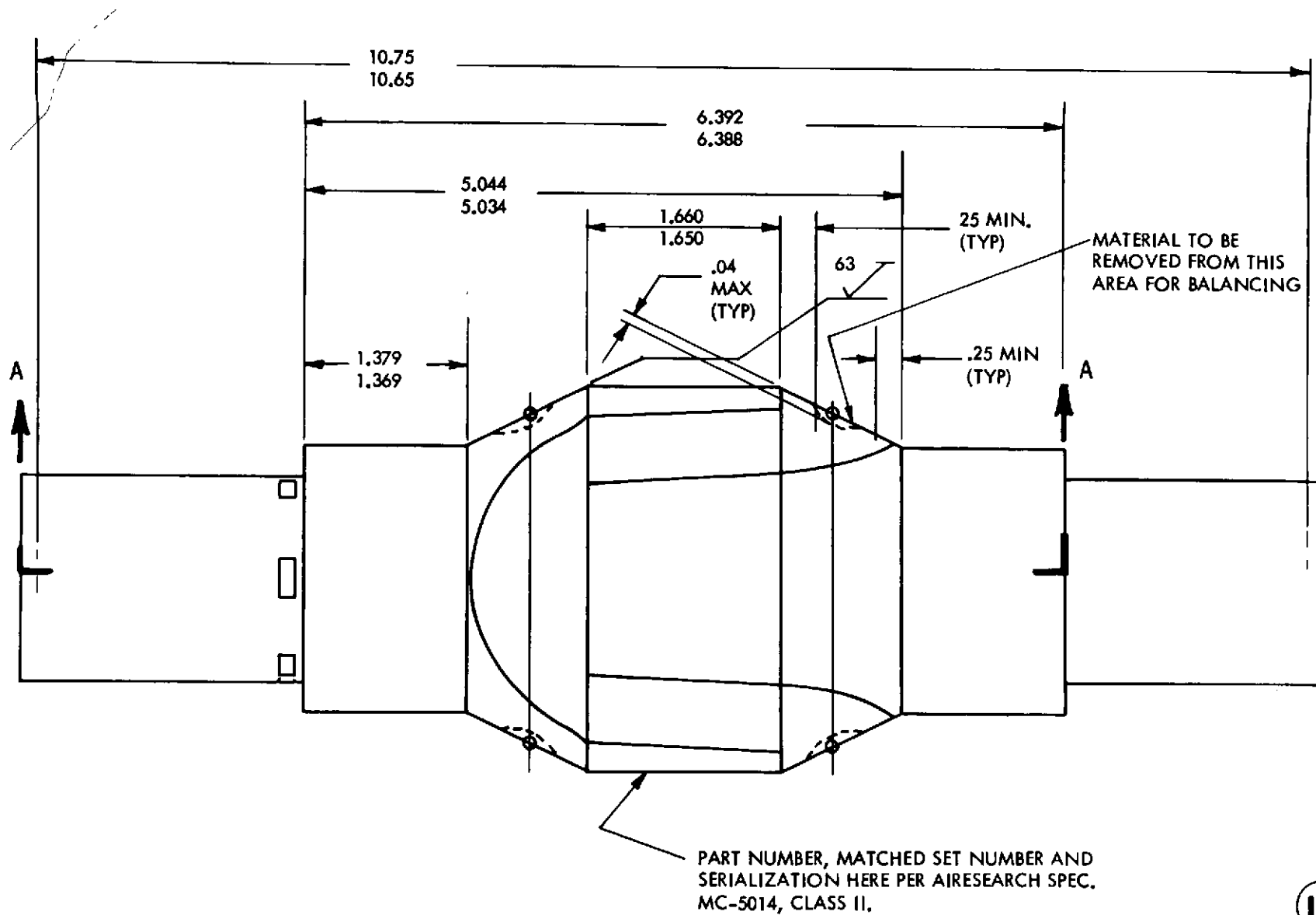


Figure 1. Outline Drawing of Finished Rotor (Reference 2)

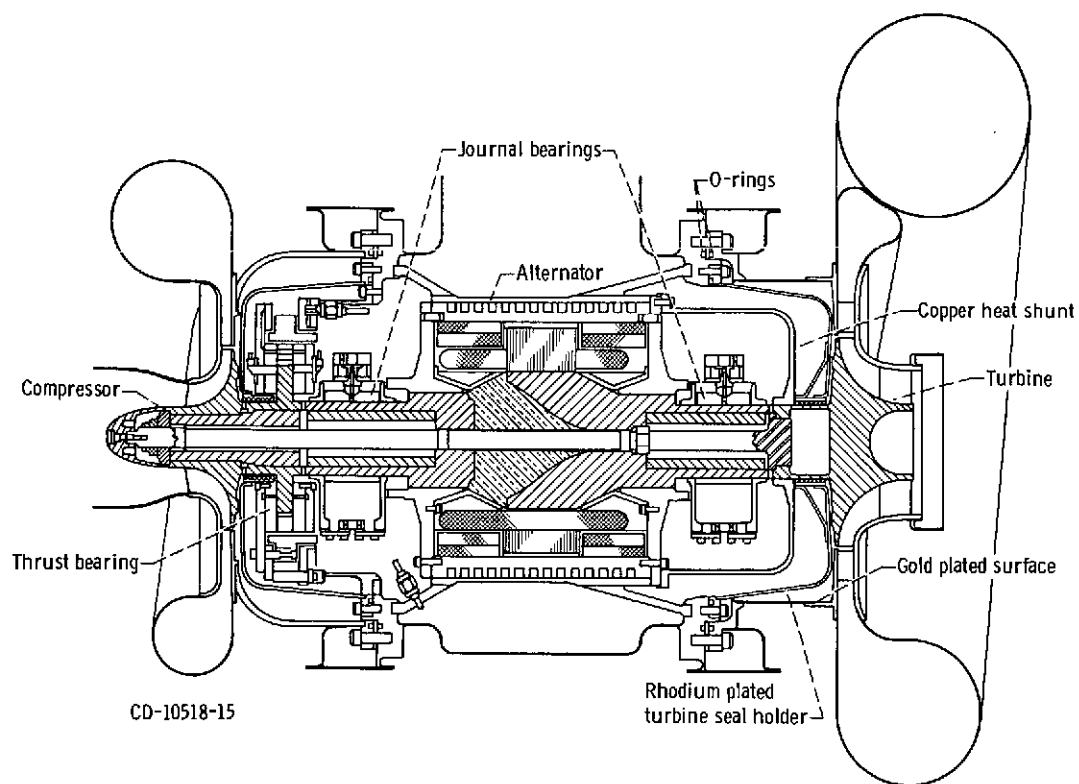


Figure 2. Schematic Drawing of Brayton Cycle Turbo Alternator-Compressor Unit  
(Reference 3)

One barrier is the uneven surface possessed by the materials to be joined. On a microscopic scale these real surfaces are very rough. For example, the most highly polished surface will still contain peaks of approximately  $500\text{\AA}$  (50nm) in height. This condition limits the area of initial contact to only a very small fraction (estimated to be about  $10^{-6}$ ) of the nominal surface area. The second barrier to welding is surface contamination. A clean metallic surface is almost immediately covered with an oxide film upon exposure to air. This film is typically several hundred angstroms in thickness. This film's formation is unavoidable when the metal is exposed to air since the chemical bonds of the surface atoms of the metal must be satisfied and do so readily by chemisorption of oxygen. In addition, atmospheric gases or solvents can become physically adsorbed on the oxide layer to provide further potential impairment to welding.

To overcome these barriers to welding, consideration must be given to a number of factors. First, movement of material at the interface is necessary to increase contact area beyond its very small initial value. HIP welding generally achieves this by mechanical deformation on a microscopic scale. At applied stresses in excess of the yield stress the required local deformation readily occurs. At pressure and temperature conditions for which the yield point is not surpassed, movement of material can still be accomplished but is dependent on creep and/or diffusion mechanisms. The primary mechanism in HIP welding is, however, the plastic deformation achieved by exceeding the yield stress of the material. In dissimilar metal joints, only the weaker material need be deformed.

The second barrier in HIP welding, surface contaminant layers, is eliminated by diffusional mechanisms. This is achieved with temperatures and times sufficient to permit dissolution of the surface contaminants into the metal. Generally these temperatures are in excess of  $0.5 T_m$ . Mechanical disruption of the surface layer during welding is of decidedly secondary importance since this mechanical working is insufficient to achieve extensive dispersion in the joint area. Hence, the mechanical properties of the surface layer are also of secondary importance in this regard. The desire to minimize this layer is however desirable since its presence hinders

welding and represents contamination in the weld area even after dissolution. In this program extensive precautions were taken and some alternate approaches were tried to minimize contaminant surface layer development. Interestingly, interdiffusion is not essential to HIP welding. This has been demonstrated by the joining of copper to tungsten metals which are essentially insoluble<sup>(4)</sup>. On the other hand, extensive interdiffusion can be a problem if the reaction zone has undesirable properties. The most common problem with dissimilar materials is the formation of brittle intermetallic compounds. In such circumstances diffusion zone thickness should be minimized and generally maintained at less than 0.0005 inch (12.7  $\mu$ m).

Other factors had to be considered in addition to these fundamental areas. The material and the peculiar design features of the Lundell rotor received special attention in planning this program and in evaluating results. The major mechanical constraints were the rotor bulk, the high strength of Inconel 718 and joint fit-up. Major metallurgical constraints existed in the form of a stable surface layer associated with Inconel 718 and dimensional changes associated with the allotropic transformation of 4340. This surface layer, while desirable for imparting high temperature oxidation resistance to Inconel 718, represents an obstacle to welding. The use of high welding temperatures was anticipated for dissolution of this layer. These temperatures were expected to be above the 4340 allotropic transformation temperature thereby complicating the mechanical aspects of joining in two ways. First, upon heating, dimensional changes would produce mismatch by a "wedge effect" between components. Second, upon cooling, dimensional changes would produce residual stresses in the welded joint. Dilatometer curves for these materials showing the extent of thermal expansion mismatch between these materials are given in Figure 3.

Consideration of these mechanical and metallurgical constraints led to the selection of special test specimen configurations which incorporated complex surfaces, intentional joint mismatch and bulk approximating that of the rotor. Reasonably thick test specimens were required to demonstrate that sufficient bulk creep or yielding to accommodate poor fit-up across large sections could be realized. In addition, the use of relatively large specimens permits demonstration of the occurrence of sufficient pressure for welding across the entire joint.

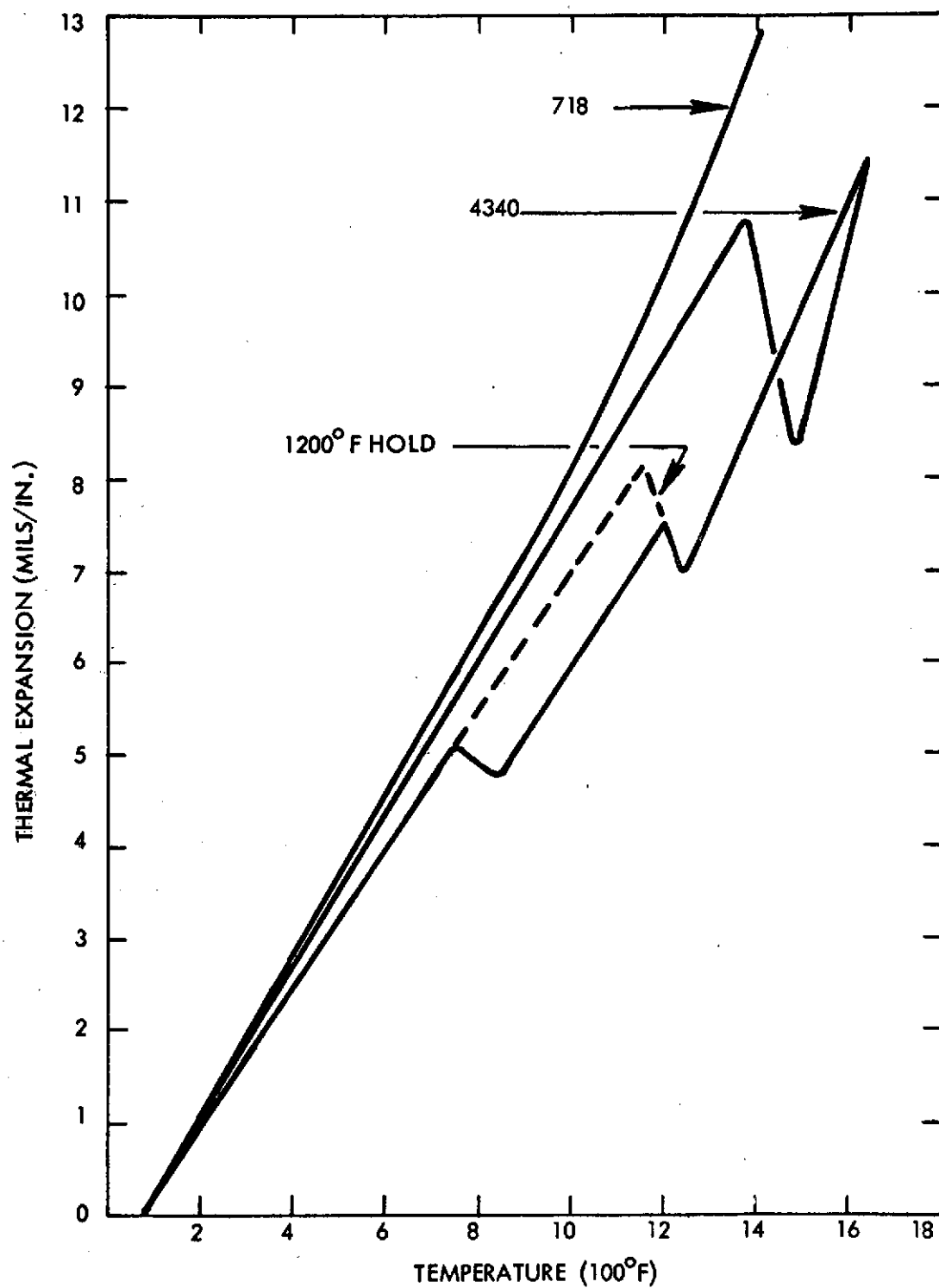


Figure 3. Dilatometer Measurement Data for Inconel 718 and AISI 4340



For the rotor application a further constraint imposed on the welding is retention, or the ability to recover, magnetic properties of the 4340. The desired properties selected were those of a coarse spheroidized structure achieved with an 8 hour (28.8 Ms) isothermal hold at 1165°F (629°C) following cooling from the austenite range. The coarse pearlite formed by this treatment is known to offer minimal resistance to domain movement. A similar isothermal treatment was readily incorporated into bonding runs providing an advantage in terms of mechanical constraints; i.e., transformation strains could be accommodated in part by creep as Fe<sub>3</sub>C spheroidization progressed. Autoclave pressure of about 28,000 psi ( $1.93 \times 10^2$  MN/m<sup>2</sup>), was maintained during this thermal arrest as a further precaution against distortion. The magnetic property requirements dictated the following modest goals for the rotor component properties in the as-welded condition:

	<u>AISI 4340</u>	<u>Inconel 718</u>
Retained Austenite (%)	<1.0	---
Min. Yield Strength (psi)	50,000	100,000
Min. Yield Strength (MN/m <sup>2</sup> )	$3.44 \times 10^2$	$6.88 \times 10^2$
Min. Tensile Strength (psi)	100,000	100,000
Min. Tensile Strength (MN/m <sup>2</sup> )	$6.88 \times 10^2$	$6.88 \times 10^2$
Min. Elongation (%)	10	

Secondary objectives identified as critical in this application were satisfied during the development phase of this program. These fell into two categories: those required for selection of rotor welding parameters, and second, those which could demonstrate growth potential for higher speed, lighter weight assemblies capable of operation under conditions of greater stress and temperature. To establish the basic rotor welding parameters the following secondary objectives were evaluated:

- o Effect of surface preparation including mechanical, chemical, and ion off-sputter cleaning. Sputter-ion plating was also investigated as a means of preserving the cleanliness achieved with the electronic surface preparation.
- o Effects of specimen pretreatment: vacuum degassing of the 4340 prior to welding and use of vacuum melted 4340.

- o Effect of joint fit-up as demonstrated by accommodation, during welding, of intentional joint mismatch. Unique specimen configurations were designed for this purpose.
- o Determine if welding could be accomplished below the  $A_{e1}$  temperature ( $1325^{\circ}\text{F}$  ( $718^{\circ}\text{C}$ )) when corrected for the weld pressure) to avoid introduction of residual stresses caused by expansion of the 4340 during its allotropic transformation from austenite.
- o Establish the ability to incorporate the allotropic transformation as an integral portion of high temperature welding cycles while maintaining autoclave pressure to help relieve transformation strains.

Additional tests were conducted to establish feasibility of utilizing this process for fabricating more advanced rotors. Modest evaluations in two additional areas were conducted for this purpose.

- o Heat treatments, following bonding and cooling to room temperature, were evaluated to determine if joint strength would be improved.
- o A high temperature magnetic material, Hiperco-50 (50Fe-50Co) was welded to 718 as a trial for potential substitution for 4340 steel in this process. More generally this effort was needed to demonstrate the applicability of the process to alternate materials.

A total of twelve welding runs were made during this program. The latter two runs each contained one rotor and a number of qualification coupons and specimens for destructive evaluation. The rotor trials utilized parameters identified as optimum within the constraints of this program. These optimum parameters were determined from an evaluation of previous trials made with sub-sized specimens. Trials on these specimens were evaluated sequentially so that redirection of emphasis occurred as test results accumulated throughout the program.

This sequence of events is not described in this report but rather the essentially definitive techniques and results are presented.

## II. EXPERIMENTAL PROCEDURES

The autoclave utilized in this program had a hot zone diameter of 7-1/2 inches (0.1905 m) and uniform temperature length in excess of two feet (0.610 m). Hence, a considerable sample load could be handled in one run. Maximum furnace temperature was 1832°F (1000°C) providing load temperatures up to 1750°F (954°C). Maximum design pressure was 30,000 psi ( $2.065 \times 10 \text{ N/m}^2$ ). All runs were made in the pressure range of 28,000 to 29,000 psi (193 to 200 MN/m<sup>2</sup>).

To determine the conditions necessary to weld the rotor components (shown in Figure 4) preliminary welding trials were made using different specimen geometries to simulate the various features of rotor components. Simple, flat-faced weld specimens (Figure 5) were used to establish baseline data. They provided means for quickly checking the extent and quality of welding since metallographic and bend strength coupons were easily removed from them.

The complex geometry of the rotor components was simulated by the weld specimens shown in Figure 6. These two specimen types were mated with known amounts of mismatch between the joint surfaces of their assembled components. Preweld mismatch gaps up to 0.015 inch (.381 mm) were utilized to simulate the mismatch conditions anticipated in actual rotor welding. Two surface configurations were provided; Type I specimens (Figure 7) were 1 inch (25.4 mm) in diameter and contained two conical interfaces per specimen, and Type II specimens (Figure 8) had sawtooth configurations, two teeth per specimen, one mismatched at the apex, the other at the base. Type II specimens are fairly bulky being 2-1/2 inches (63.5 mm) in diameter. These specimens are inherently self locking in configuration, and thus require considerable metal flow to accommodate mismatch during welding.

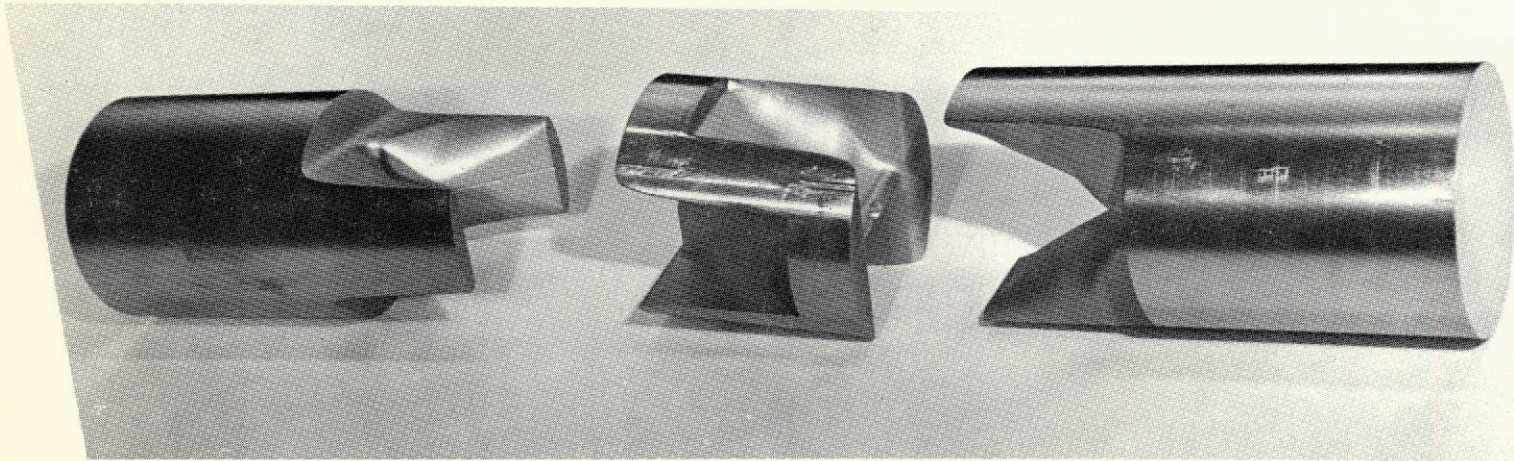
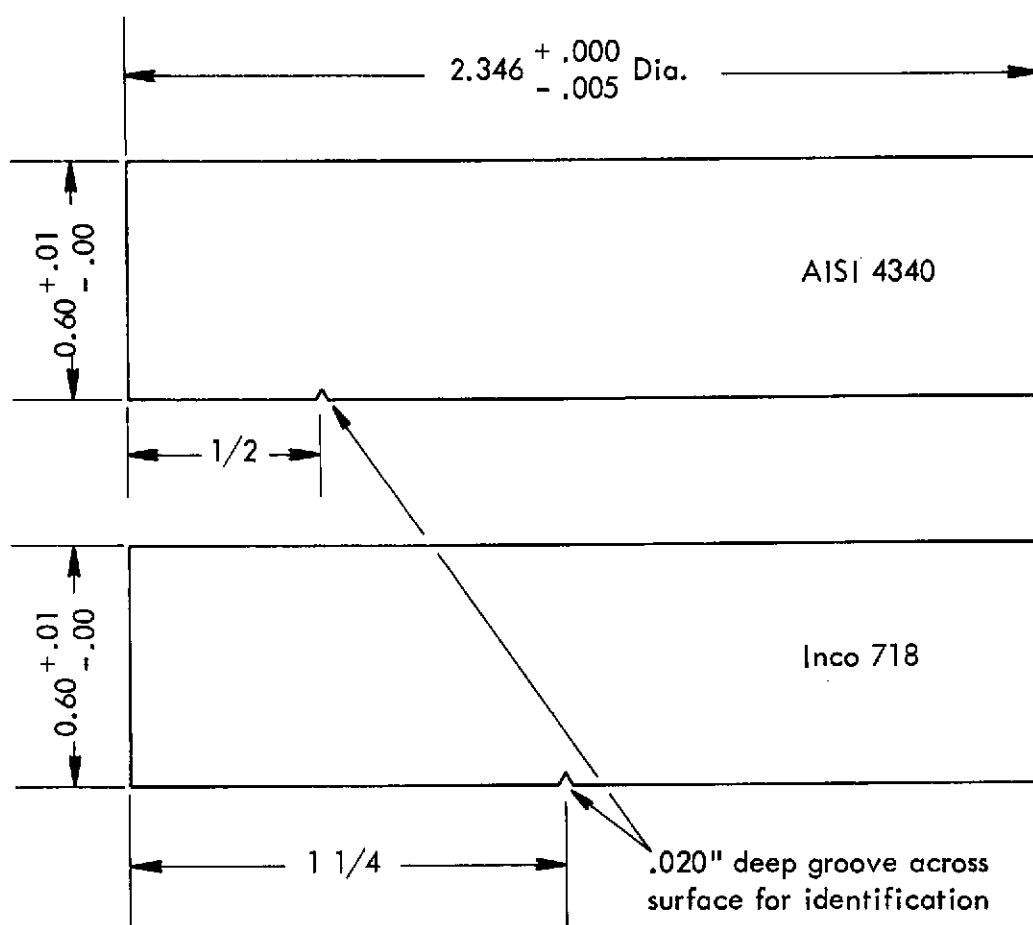


Figure 4. Rotor Blank Components Prior to HIP Welding



Note - All flat surfaces to be parallel within .001 (Top to bottom and piece to piece).

Figure 5. Simple Weld Specimen



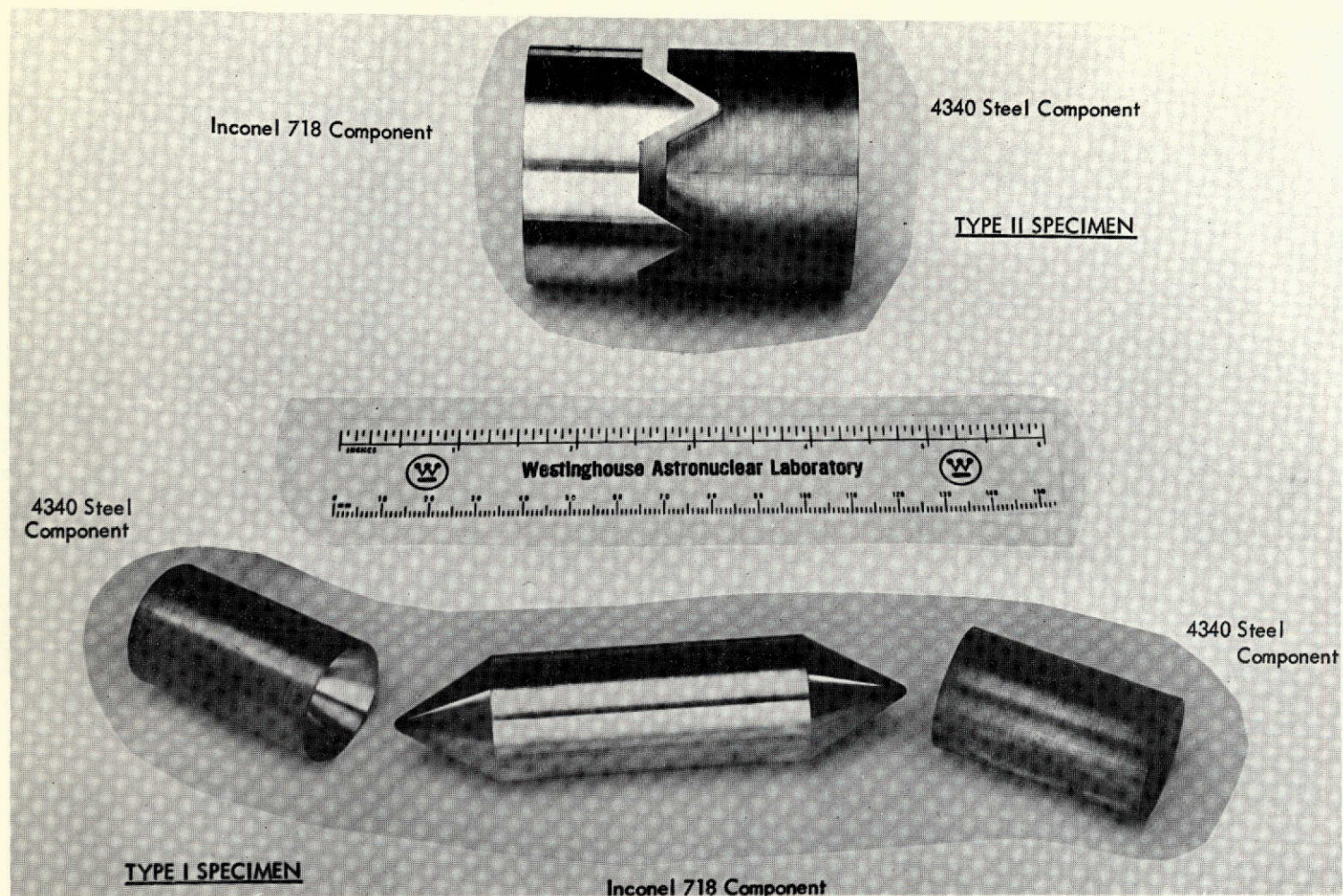


Figure 6. Complex Weld Specimens

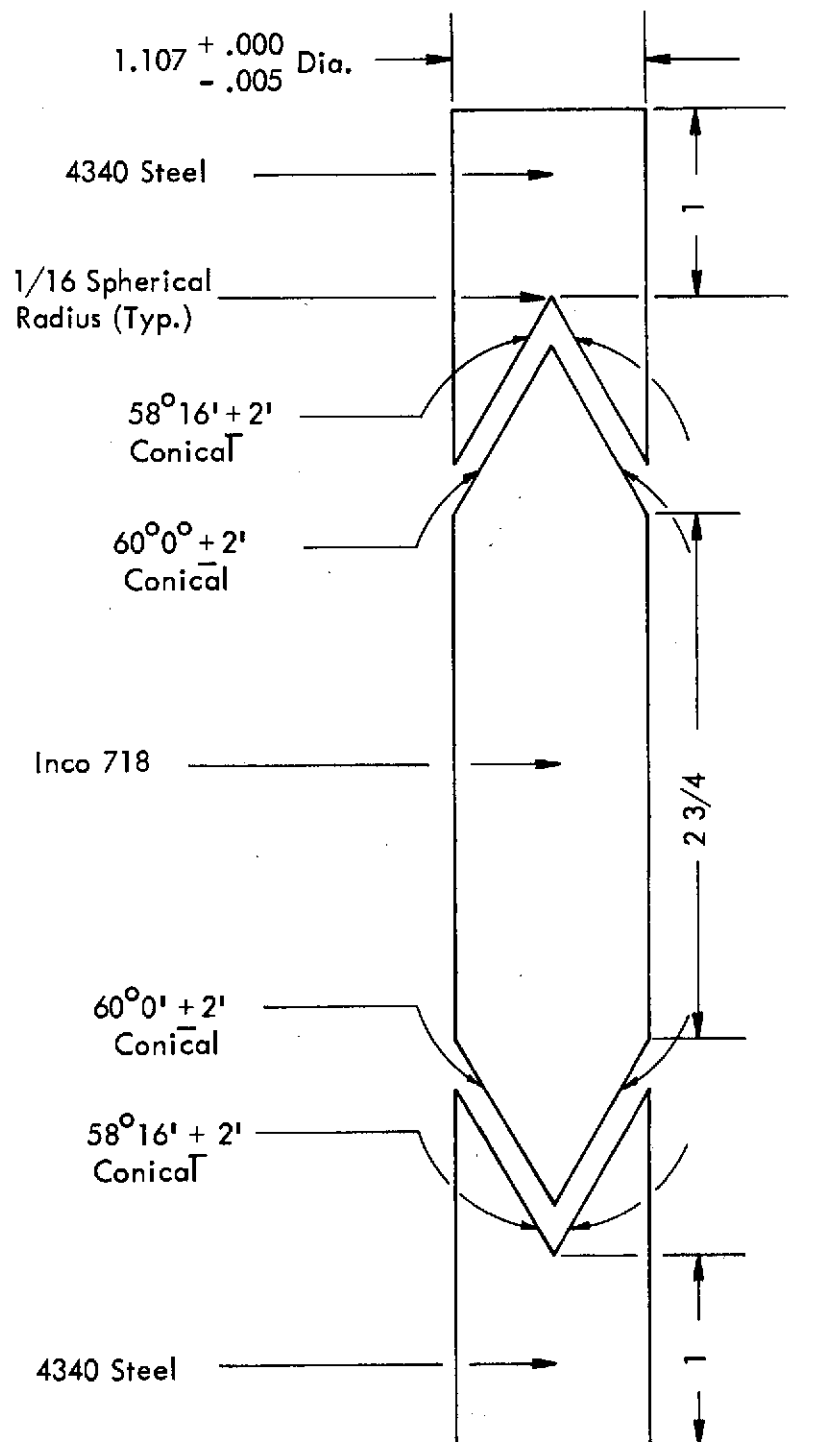
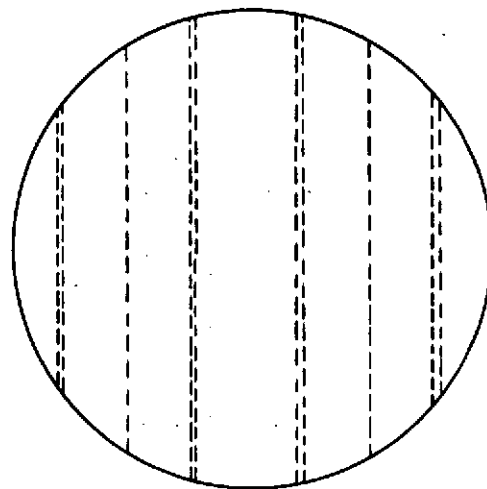
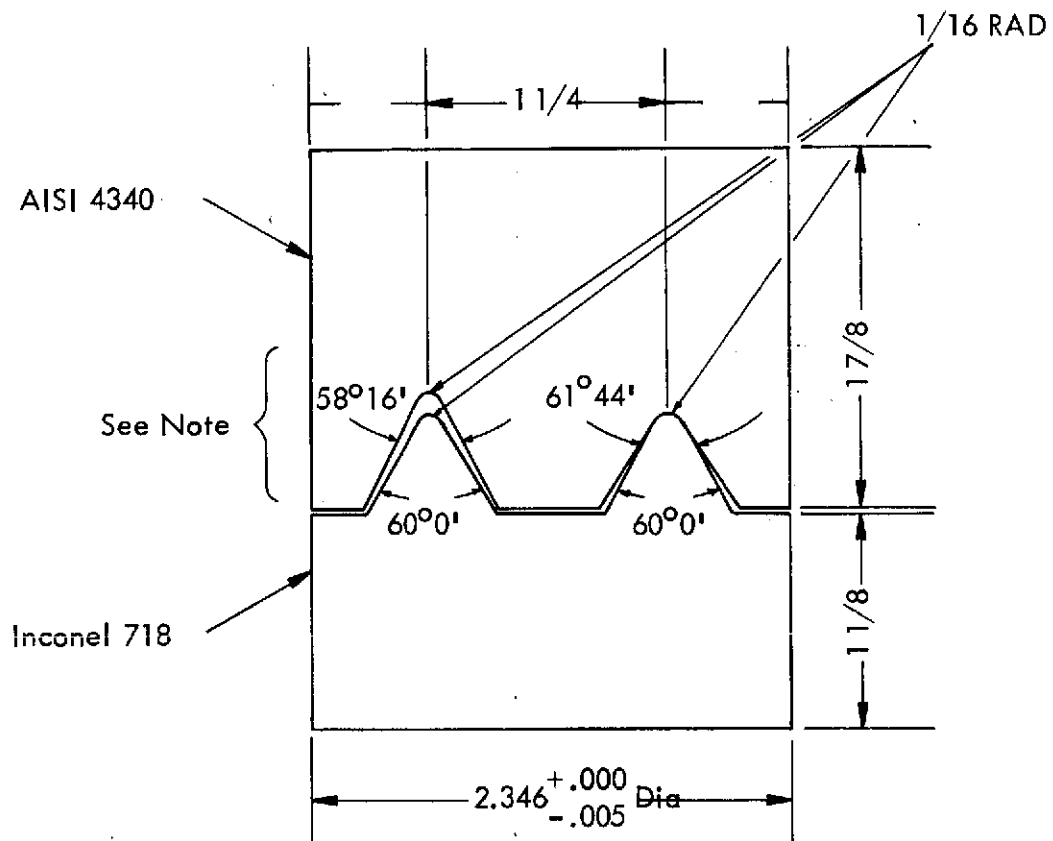


Figure 7. Type I Mismatch Specimen





Bottom View

Note - Tolerance on these angles is  $\pm 2'$

Figure 8. Type II Mismatch Specimen

Stainless steel (Type 304 ) was used as the canning material. Cans for the weld specimens were comprised of spun end caps tightly fitted into the ends of thin walled tubes. Figure 9 is a sketch of an end cap used in forming a can for HIP welding Type II specimens. Rotor cans were joined by seam welding sheet which was tightly wrapped about the circumference of the assembled rotor. Spun end caps were also used for these cans. A number of uncanned evaluation specimens were included in each autoclave run. These specimens included Rowland rings (Figure 10) for the measurement of magnetic permeability and tensile and charpy blanks from which post-weld strength properties of the rotor materials could be determined. A photograph of several of each type of evaluation specimen is presented in Figure 11.

Inconel 718, bar, obtained in the hot rolled and annealed condition, was heat treated to give it maximum ductility and minimum strength for welding. This treatment consisted of solution treating for 3 hours (10.8 ks) at 1800-1850°F (982-1010°C), furnace cooling to 1450-1500°F (798-815°C) and holding for 24 hours (86.5 ks) followed by furnace cooling to room temperature. Later in the program this anneal was deemed unnecessary since joint compliance is easily achieved by deformation of the 4340. Consequently, the rotor was welded with the 718 in the as-cast condition.

The requirement of high magnetic permeability dictates that the 4340 steel portion of the rotor possesses a coarse spheroidized microstructure. Since the preliminary welding trials were planned to be made above the  $A_{e3}$  temperature, the 4340 steel required no heat treatment but rather was left in the as-received hot rolled and annealed condition.

In several instances weld specimen components of Hiperco-50 were substituted for 4340 steel components to allow the welding behavior of the former material with Inconel 718 and joint strength to be determined. The Hiperco-50 was not heat treated to enhance its strength or magnetic properties.

Material: 304 Stainless  
2B Finish  
20 Gage (.037 thick)

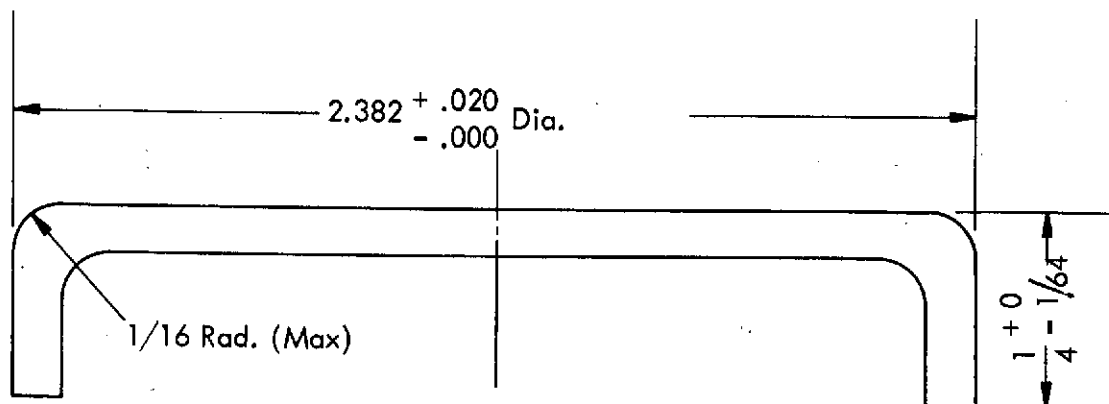
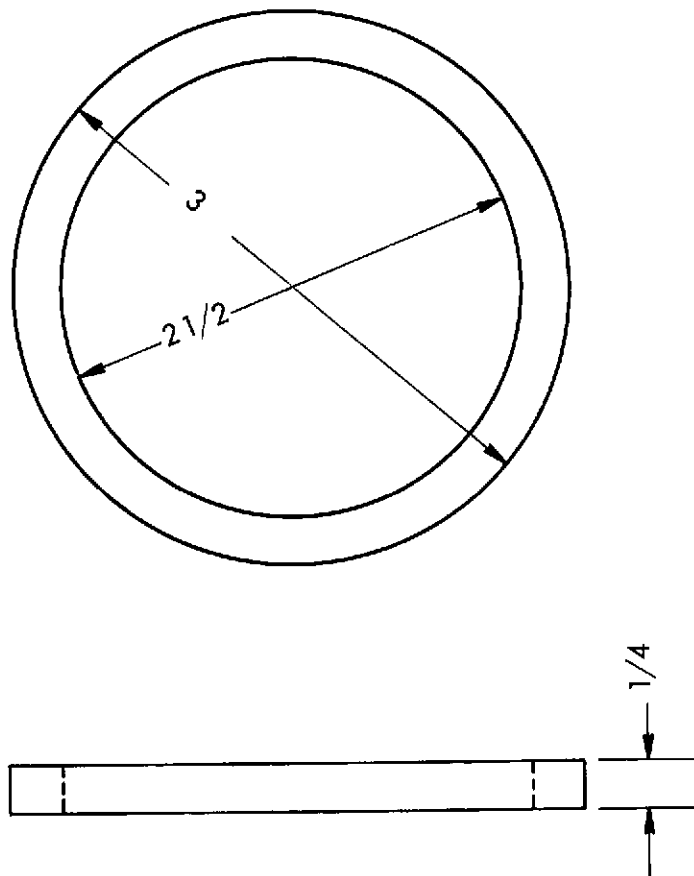


Figure 9. End Cap for Can Used in HIP Welding



Material: AISI 4340 Steel

Note - Tolerance on all dimensions  $\pm \frac{1}{64}$

Figure 10. Rowland Ring Specimen

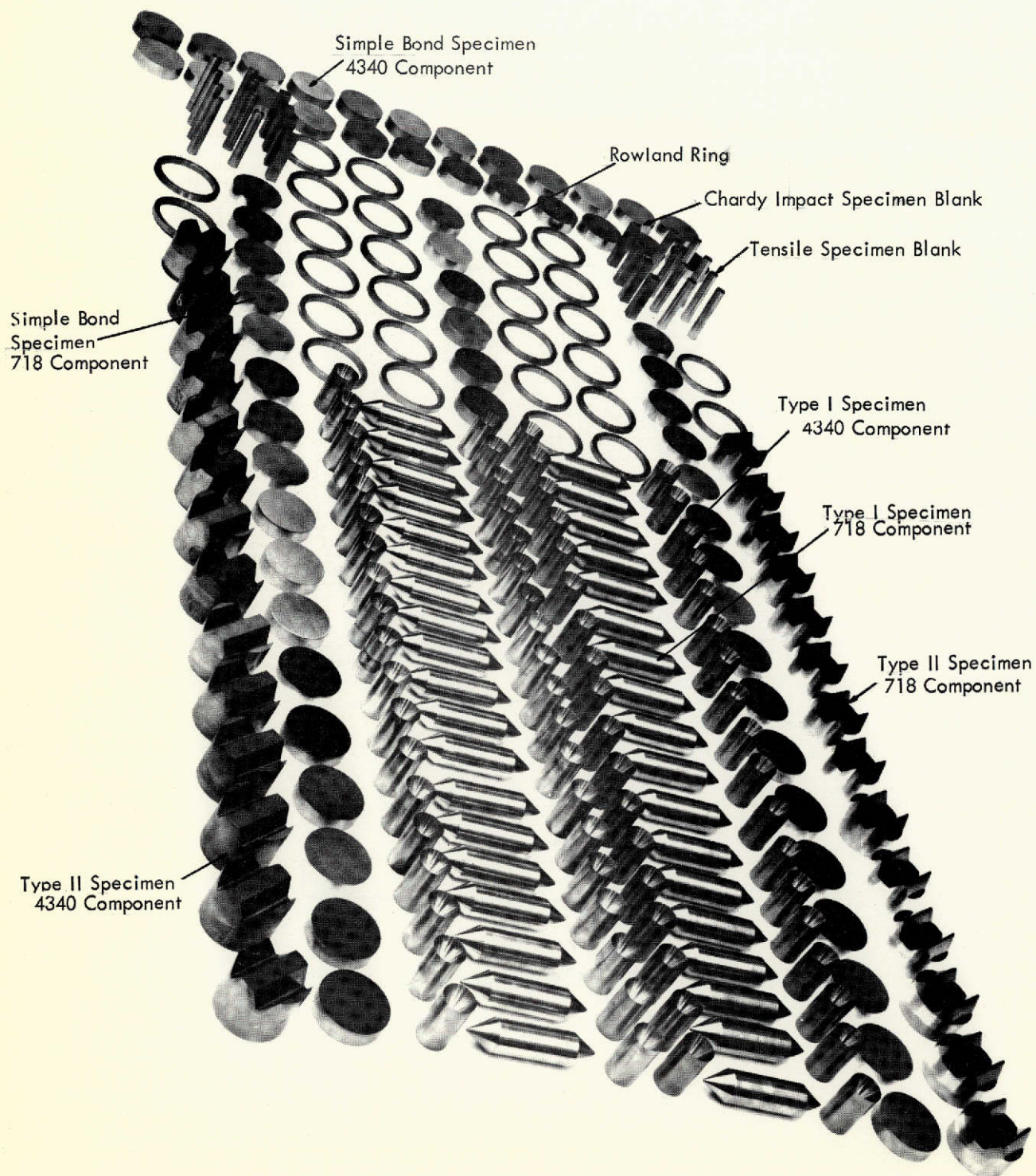


Figure 11. Photograph of Portion of Specimens Used in Experimental Program

Various surface preparations were used on the weld specimen components. A number of specimens were sputter ion coated with gold in high vacuum. The clean, plated surfaces were thus protected from reaction during subsequent exposure to air. The initial stage of this coating process consisted of off-sputtering the surface of the specimens. This was accomplished by applying a bias RF voltage to the substrate to sputter material from the substrate surface. The removed material was collected by the shutter placed between the substrate and the pure metal target. This was followed by sputter-ion plating producing an adherent film of approximately  $250\text{\AA}$  (25 nm) in thickness.

Another portion of the weld specimens were chemically etched in aqueous acid solutions and thoroughly cleaned. The etching procedure was as follows:

4340 steel components: 10% HCl at  $100^{\circ}\text{F}$  for approximately 5 minutes (300 s)

718 Inconel components: 30%  $\text{HNO}_3$  + 5% HF for approximately 0.5 minute  
(30 s)

Hiperco-50 components: 25% HCl + 5%  $\text{HNO}_3$  + 2-1/2%  $\text{H}_2\text{SO}_4$  for approximately  
1 minute (60 s)

Cleaning consisted of the following operations:

- a. Scrub with hot tap water and abrasive type detergent (principal active ingredient is trisodium phosphate).
- b. Rinse with hot tap water.
- c. Rinse with boiling distilled water.
- d. Spray rinse with grain alcohol.
- e. Air dry.

Personnel handling the cleaned components wore pre-scrubbed, pure latex gloves. Direct contact with specimens during storage was made only with Kimwipes or laboratory blotter paper.

In addition, it was shown that a vacuum degassing treatment of 24 hours (86.5 ks) at 1800°F (982°C) and  $10^{-5}$  torr ( $1.3332 \text{ mN/m}^2$ ) was required for proper preparation of 4340 components.

Prepared weld specimens and identified cans were given an overnight pumpdown in a GTA weld box. The specimens were loaded into the cans following backfilling of the box with ultra pure helium. The lids of the cans were fusion arc welded in place with a small evacuation hole left unwelded. The welded cans were transferred to the EB weld chamber and given a second overnight pumpdown before being sealed by electron beam welding. The sealed cans were leak tested by immersion in methanol following helium pressurizing for 20 minutes (1.2 ks) at 400–500 psi ( $2.76\text{--}3.45 \text{ MN/m}^2$ ) in a room temperature autoclave. Where bubbles were noted the cans were resealed by EB welding and again leak tested to ensure a leak free assembly.

Chromel–alumel thermocouples were attached to the sealed cans which were then loaded into a 3-3/4 inch (95.3 mm) by 36 inch (914.4 mm) long cylindrical copper autoclave fixture. The remaining volume of the fixture was filled with granular alumina as was the autoclave after loading the fixture. Once in the autoclave, baffles were placed above the fixture to minimize convection currents and thereby improving temperature uniformity. The success of this approach is evidenced by the achievement of only a 23°F (13°C) temperature gradient over the 24 inch (609.6 mm) stack height at the highest temperature of operation, nominally 1750°F (954°C).

Schedules of the parameters for HIP welding are included with the results presented in the next section of this report. All cans were leak checked after autoclaving as described previously. Machining was used to remove the cans from the specimens. Specimens which then passed dye penetrant testing on the exposed interface were selected for further destructive evaluation.

Bend test coupons were machined from the flat-faced specimens. The geometrical relation of a bend coupon to a simple weld specimen is shown in Figure 12. The coupons were bent with three point loading using a 0.12 inch (3.05 mm) radius punch applied to the weld interface while the coupon was supported over a 3/4 inch (19.05 mm) span. Bend testing was performed at ambient temperature using a 1.0 inch/minute (0.423 mm/s) crosshead speed.

Type II weld specimens were machined as shown in Figure 13 to yield tensile blanks and metallographic specimens. Tensile blanks were then machined into tensile specimens of 0.179 inch (4.55 mm) gage diameter and 2.000 inch (50.8 mm) gage length (Figure 14). The location of the blanks in the weld specimens was such as to represent pre-weld interface mismatch gaps of .002 inch (50.8  $\mu\text{m}$ ) for blank No. 2 and .004 inch (101.6  $\mu\text{m}$ ) for blank No. 3. Type I weld specimens were first cut in half lengthwise. Tensile blanks and metallographic specimens were machined from each half according to the layout of Figure 15 and 16. These tensile blanks represented pre-weld interface mismatch gaps of .009 inch (228.6  $\mu\text{m}$ ) for blank No. 2 and .006 inch (152.4  $\mu\text{m}$ ) for blank No. 3. All tensile tests were conducted at ambient temperature with a crosshead speed of 0.01 inch/minute (4.23  $\mu\text{m/s}$ ).

Rowland rings were given a D C magnetic test to assure basic compliance with magnetic requirements. For some bonding trials, a determination of Rockwell C hardness was used as a measure of magnetic permeability since both properties are a function of the degree of coarseness of the spheroidized  $\text{Fe}_3\text{C}$  in the steel. The rings were tested using a magnetizing force (H) of from 5 to 200 Oersteds (.398 to 15.920 mA/m). Values of the induced magnetism (B) were obtained and used to determine the magnetic permeability (B/H). The criterion for magnetic permeability was arbitrarily chosen as that value corresponding to an applied magnetizing force of 100 Oersteds (7.960 mA/m). This value was compared to that found for the ring specimen which had been austenitized and then spheroidized for 8 hours (28.8 Ms) at 1165°F (629°C). The value for this specimen (18 kilogauss) (1.8 T) was taken as the value to which



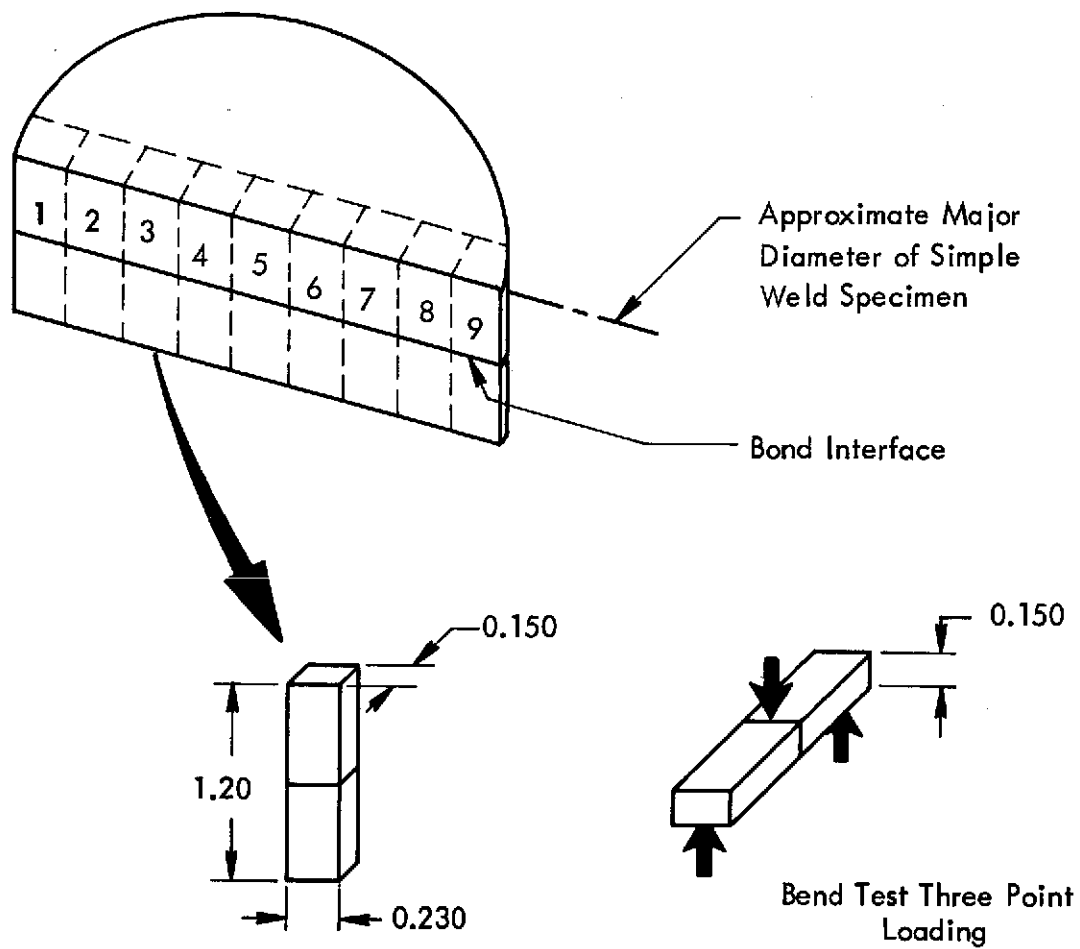
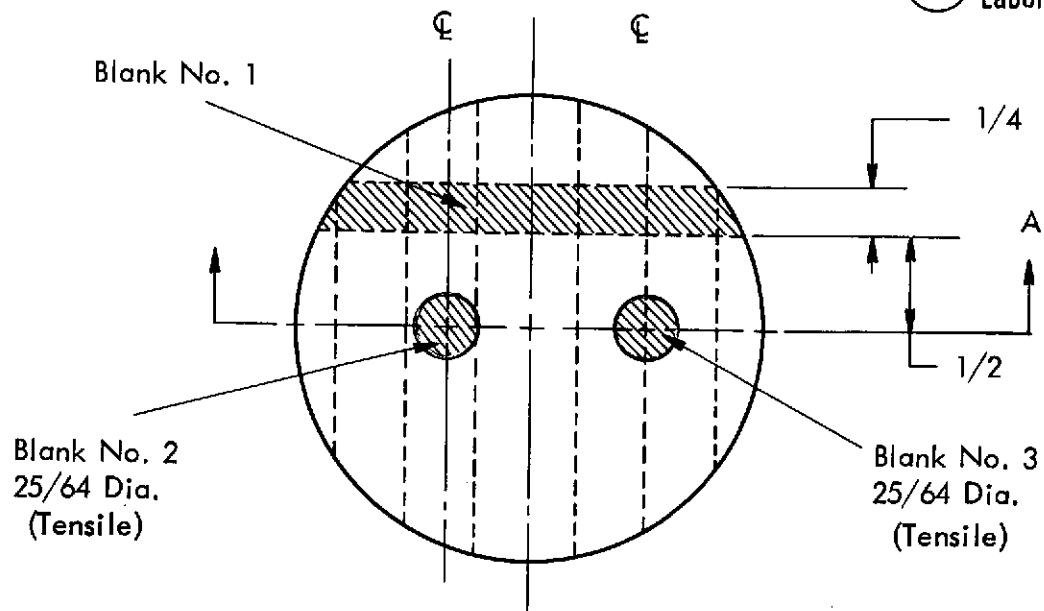


Figure 12. Geometric Orientation of Bend Coupons Machined from Simple, Flat-Faced Specimen. Transverse Section Through Welded Specimen is Portrayed.



NOTE: All dimensions  $\pm 1/64$  except where noted otherwise.

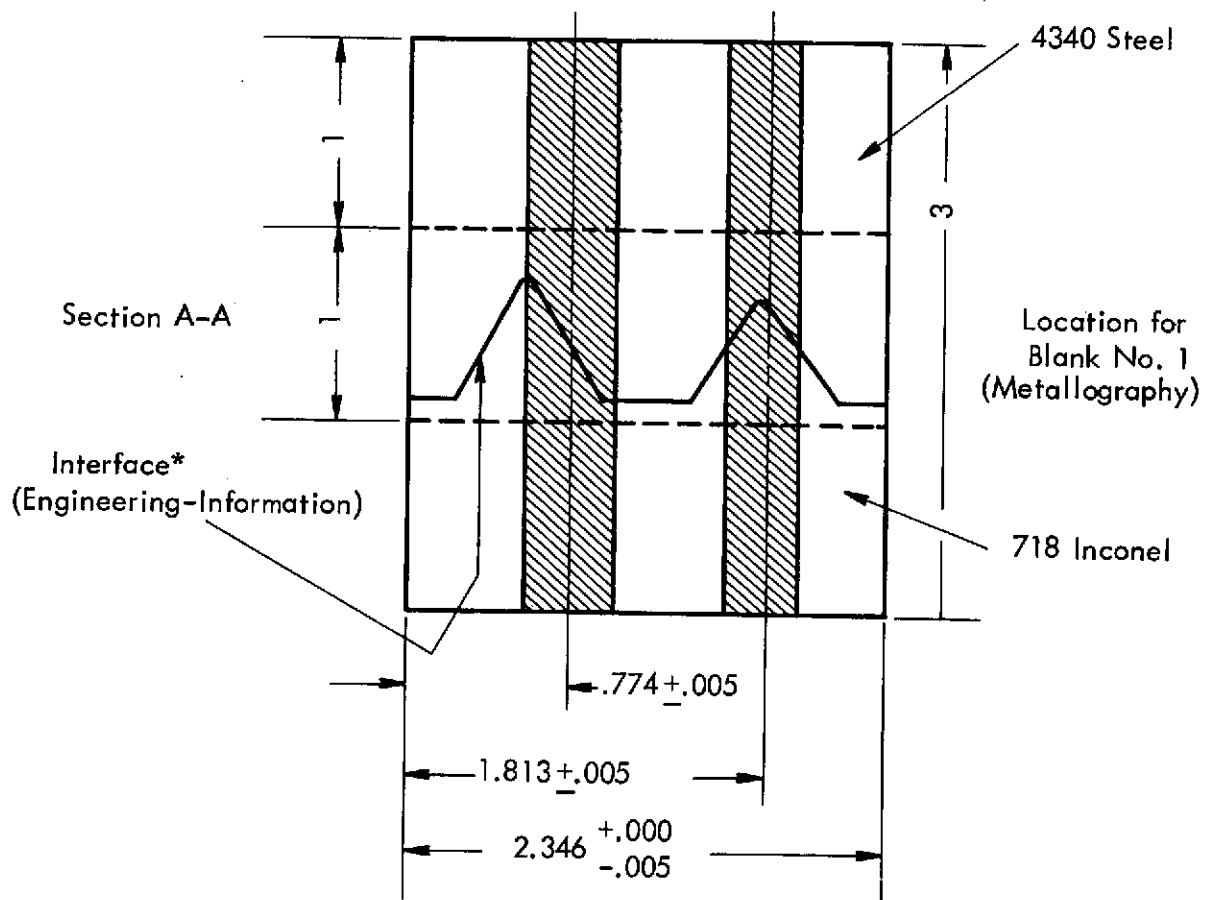


Figure 13. Sketch Showing Location of Tensile and Metallographic Specimen Blanks Within Welded Type II Mismatch Specimen.

Eccentricity between end centers not to exceed 0.0005

Figure 14. Weld Joint Tensile Specimen

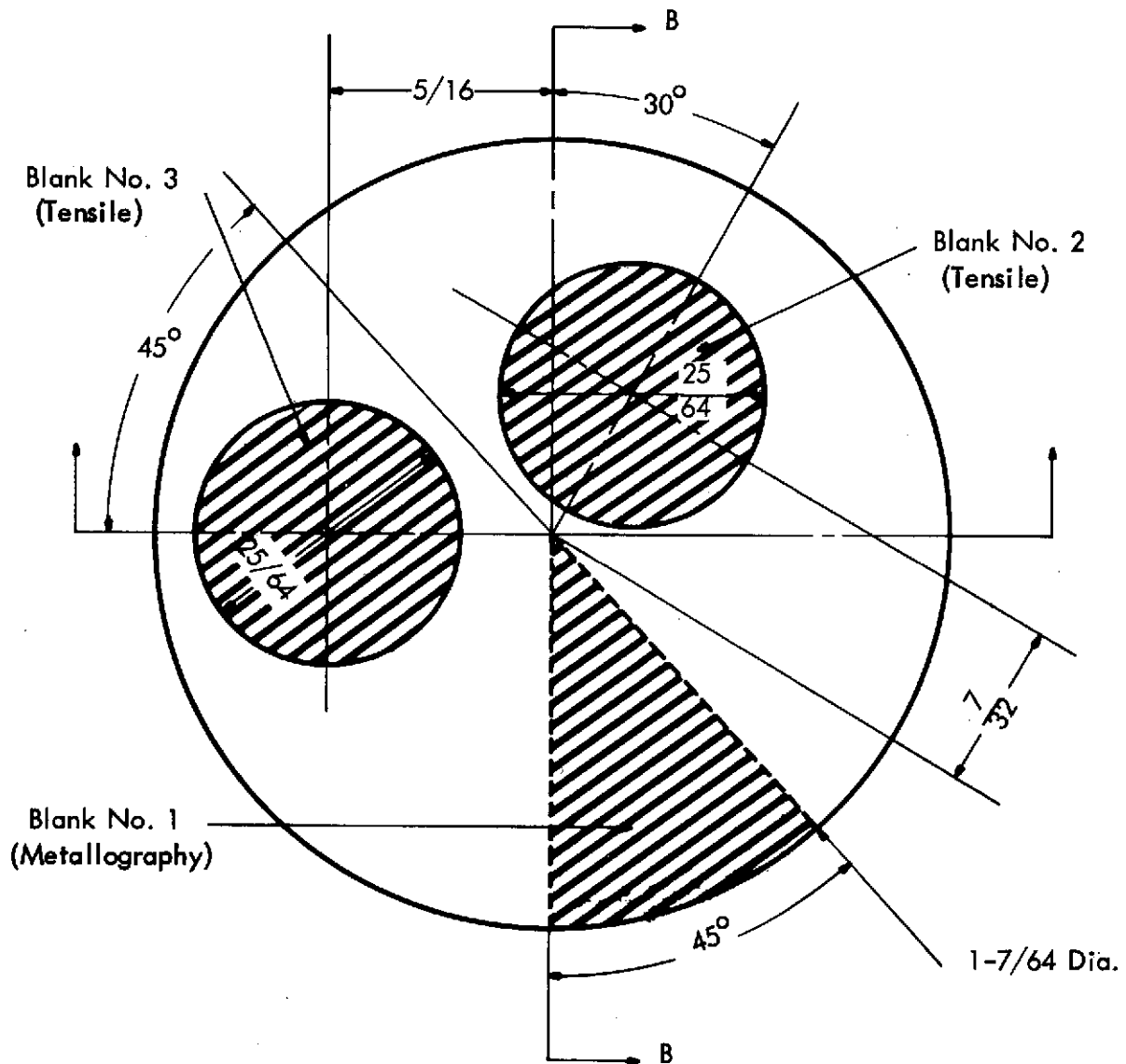


Figure 15. Sketch Showing Location of Tensile and Metallographic Specimen Blanks Within Welded Type I Mismatch Specimen.

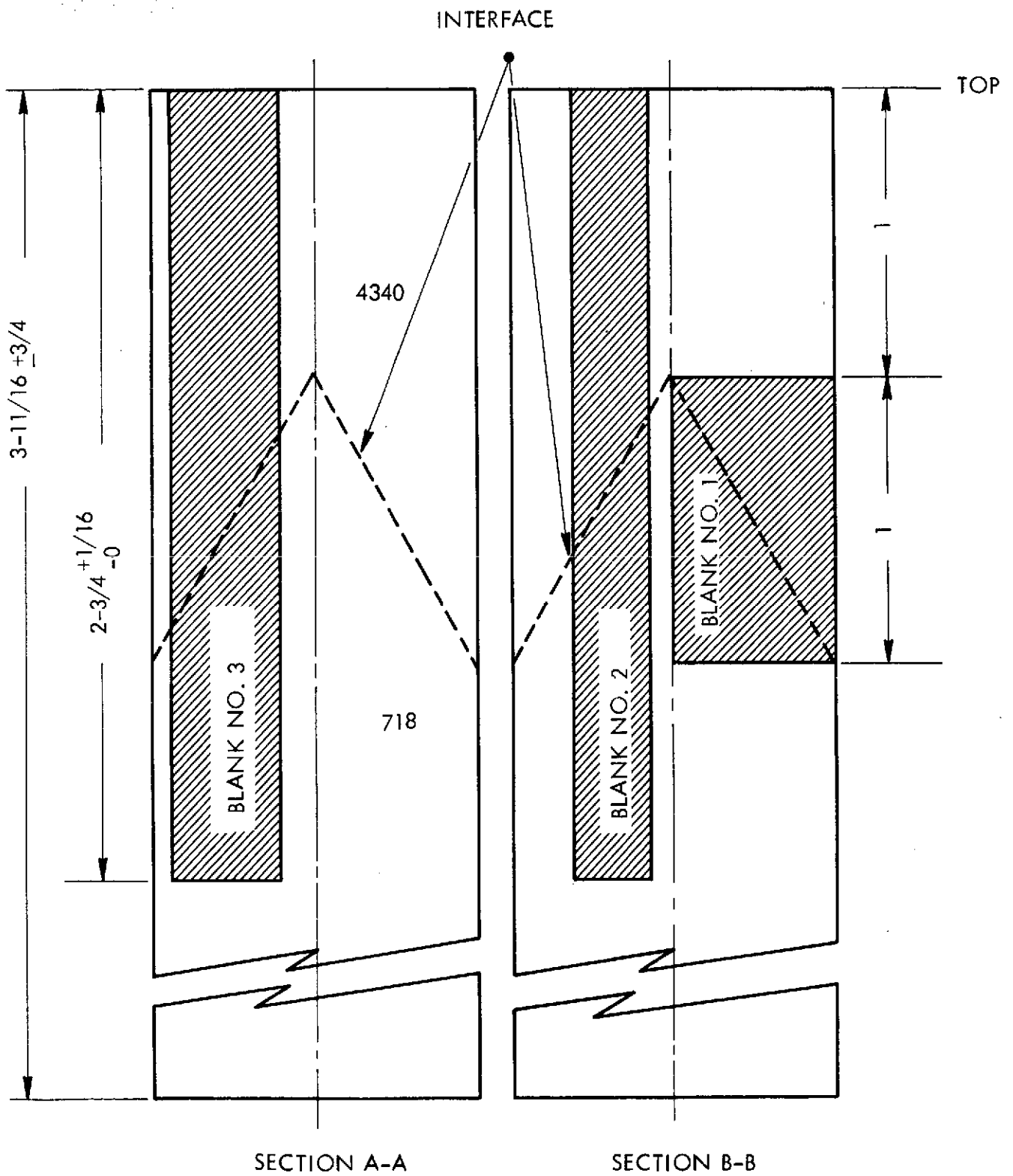


Figure 16. Sections A-A and B-B of Figure 15.

all others (those contained in the preliminary and rotor welding trials) could be compared. This specimen thus served as a "standard" for magnetic permeability. Rockwell C hardnesses were also obtained on each Rowland ring specimen.

## IV. RESULTS AND DISCUSSION

### A. Rotor Welding

Two full size rotors were successfully HIP welded utilizing parameters which, within the limits of this investigation, were optimized during the course of the preliminary weld trials. One HIP welded rotor blank with its stainless steel can partially machined off is shown in Figure 17. The HIP weld schedule for these units was as follows:

Components were prepared for welding by cleaning and etching as described on page 21. In addition, the AISI 4340 pole pieces were vacuum degassed at  $10^{-5}$  torr ( $1.3332 \text{ mN/m}^2$ ) and  $1850^\circ\text{F}$  ( $1010^\circ\text{C}$ ) for 24 hours (86.5 ks) prior to canning.

Welding was accomplished by holding at  $1730 \pm 20^\circ\text{F}$  ( $944 \pm 11^\circ\text{C}$ ) for 4 hours (14.4 ks) at 29,000 psi ( $200 \text{ MN/m}^2$ ).

A spheroidization heat treatment was incorporated during cooldown by holding at  $1200^\circ\text{F}$  ( $650^\circ\text{C}$ ) for 12 hours (43.25 ks) while maintaining 29,000 psi ( $200 \text{ MN/m}^2$ ) pressure.

Dye penetrant inspection showed this joint to be free of visible defects. In addition, verification specimens were included in the rotor welding run which were destructively evaluated to check the adequacy of the welding cycle. Bend fracture strengths were obtained from these specimens and are presented in Table I.

A photomicrograph taken of the weld interface of one of the specimens is presented in Figure 18. Excellent interfaces were found for each specimen. Values for the  $R_c$  hardness given in Table I are indicative of greater than 96% of the magnetic permeability of the "standard" magnetic specimen which, as noted previously, attained an induced magnetism of 18.0 kilogauss (1.80T) with a magnetizing force of 100 oersteds (7.960 mA/m).



Figure 17. HIP Welded Rotor Blank. Canning Material has been Machined on Central Section.



Table 1. Bend Fracture Strength Results Obtained from Rotor Verification Specimens\*

Specimen No.	Associated Rotor No.	Average Bend Strength (psi)	Average Bend Strength (MN/m <sup>2</sup> )	Fracture Description	Rc of 4340 Portion
YSC	1	128,500	885	ductile, occurs through Inco 718	12
YSCR	1	128,600	886	"	14
ZSVC	2	119,700	825	"	13

\* The test data from which this table was prepared are contained in Appendix A, pages 13-15.

Reproduced from  
best available copy. 



718

4340

400X

Figure 18. Weld Interface of Verification Specimen HIP Welded with Rotor Blank.

As noted previously, the welding parameters and materials preparation procedures used to successfully weld the rotor components were those found by evaluation of the results of preliminary welding trials to be optimum. The significant results obtained from the evaluation of these preliminary trials are presented in the balance of this discussion. In each case data is shown and compared with corresponding data for the selected rotor welding parameters. The basis for selection of rotor welding parameters is reviewed, and the adequacy of this selection is demonstrated.

#### B. Outgassing of 4340

The variable having a most significant effect on HIP welded joint performance was outgassing of the 4340 steel component which is illustrated by the test results in Table 2. Consistently high joint strengths were obtained when the 4340 was vacuum outgassed prior to welding. Failure to do so resulted in erratic behavior with joints exhibiting very low to very high strength.

The erratic behavior of joints containing non-outgassed 4340 can be attributed to the character of the inter-diffusion zone formed during the HIP welding.

As shown in Figures 19a, the interdiffusion zone formed between outgassed 4340 and 718 appears single phase while the interdiffusion zone between non-outgassed 4340 and 718 is two phase (Figure 19b). Microhardness transverses revealed that this thin layer adjacent to the 718 is extremely hard (see Figure 20), and it is through this hard brittle layer where joint failure was observed to originate. From these results it is evident that the source of interface

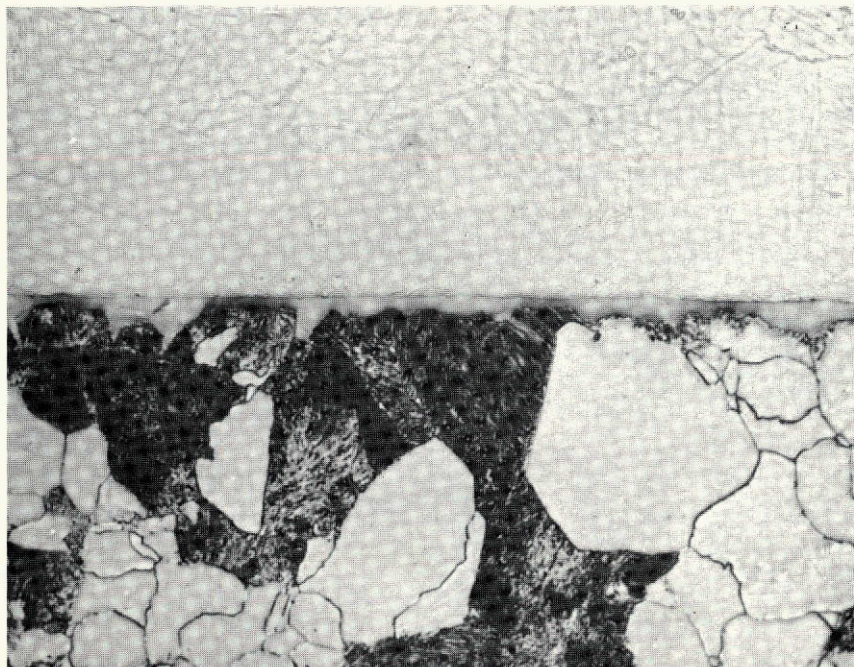
Table 2. Comparison of Tensile Strengths of Welds Prepared with Specimens Containing Outgassed and Non-outgassed 4340 Steel\*

Ultimate Tensile Strength of Specimen Weld (psi)			
Outgassed 4340		Non-outgassed 4340	
(psi)	(MN/m <sup>2</sup> )	(psi)	(MN/m <sup>2</sup> )
75,900	523	71,840	495
76,000	524	72,560	501
83,800	578	95,400	657
84,600	584	98,200	677
92,500	638	**	
98,800	681	**	

\* The test data from which this table was prepared are contained in Appendix A, pages 5-7 for the outgassed material and pages 9-11 for the non-outgassed material.

\*\* Tensile specimens fractured during machining.



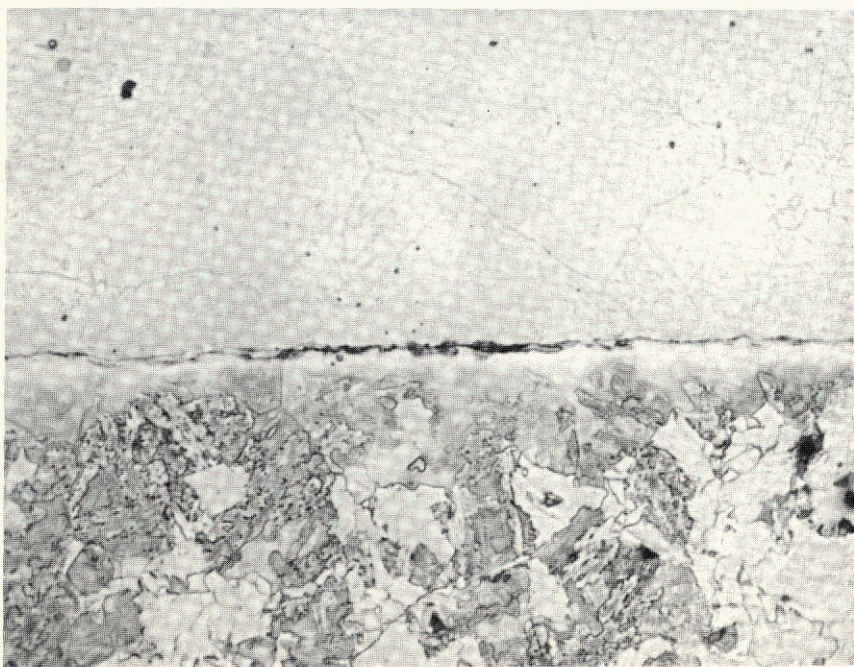


718

4340

400X

a) Outgassed 4340/718 HIP Welded Joint



718

4340

400X

b) Non-outgassed 4340/718

Figure 19. Photomicrographs of HIP Welded 4340/718 Joints

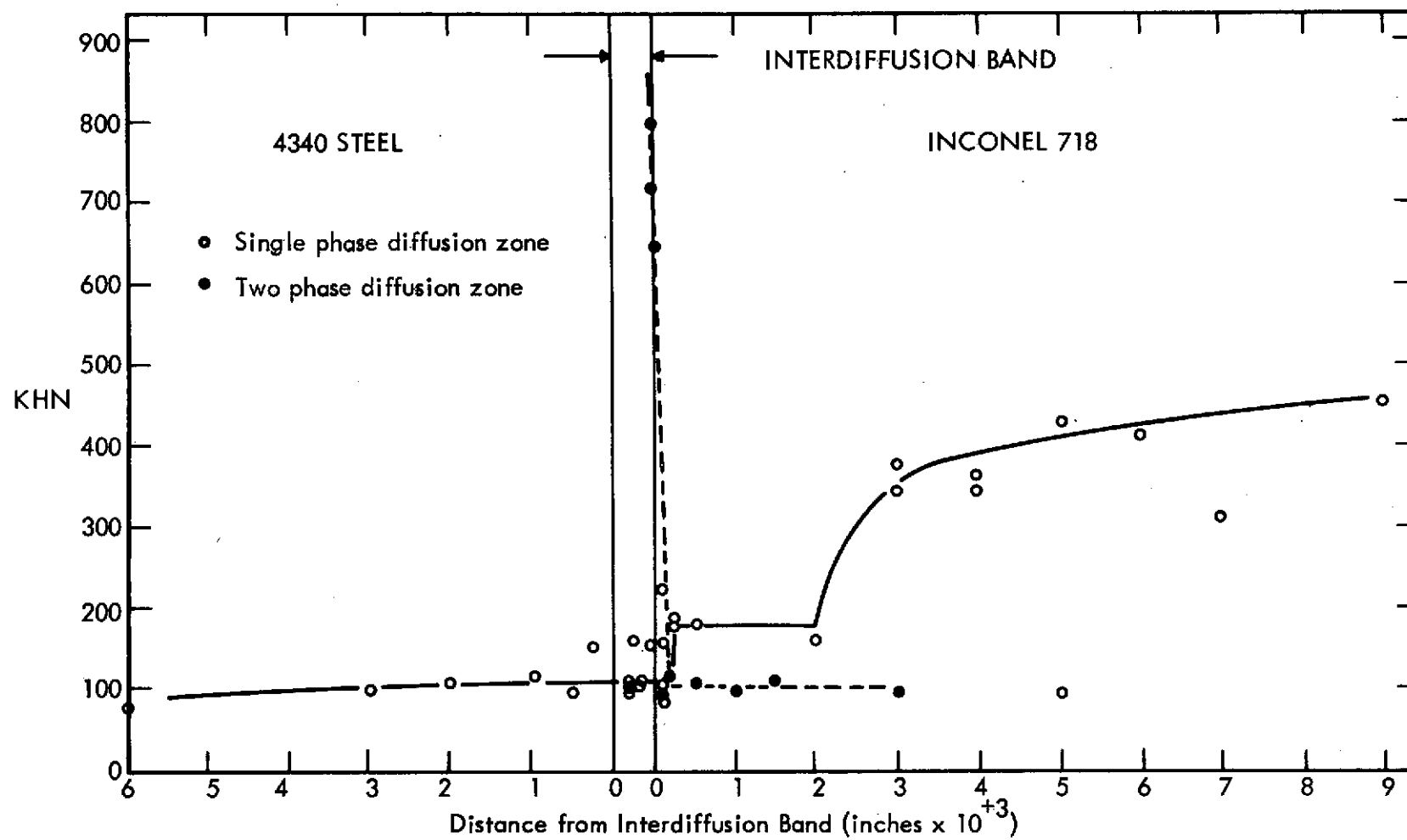


Figure 20. Microhardness Traverses of 4340/718 HIP Welded Joint

contamination is transfer, during specimen heating, of volatile contaminants from the 4340 to the surface of the Inconel 718. Consistently strong welds can be achieved when this outgassing is accomplished prior to canning.

No significant difference in weld joint strength was observed when vacuum melted 4340 steel was substituted for non-vacuum melted stock (see Table 3). However, both varieties were vacuum outgassed prior to joining. Thus, any difference in content of volatiles that would impair welding was most likely negated by the vacuum outgassing operation. Tensile specimens tested from HIP welds of each 4340 material to Inconel 718 demonstrated that joint ductility was possessed for each material combination. Tensile failure occurred first through rupture in the base metal region of the 4340 and was followed by interface failure. Evidence for this mode of failure is shown in Figure 21 which compares a tensile specimen exhibiting ductile failure with one that failed entirely along the original interface.

### C. Surface Preparation

Data on joint tensile strengths were obtained as a function of surface preparation method. For this comparison the other pre-weld and weld variables were those used to weld the rotors except that several specimens were held at the welding temperature for several hours longer. This deviation is shown in a subsequent section to have no affect on weld quality. From the data of Table 4 it is apparent that either cleaning and etching or cleaning alone is associated with high weld strength while gold coating (prior to outgassing) can produce weak welds.

Perhaps the low weld strengths associated with the gold coating are the result of the steel surface's inability to outgas through the gold. Had the gold been applied after outgassing, it may have proven beneficial. The tensile strength of gold coated specimens vary from a

Table 3. Joint Strengths of Welds Employing Vacuum Melted Steel Compared to Ones for Non-vacuum Melted Steel\*

Steel Type	Average Ultimate Tensile Strength		Average Bend Fracture Stress	
	(psi)	(MN/m <sup>2</sup> )	(psi)	(MN)
Vacuum melted	102,900	710	119,700	824
Non-vacuum melted	95,700	660	128,500	886

\* The test data from which this table was prepared are contained in Appendix A, pages 5, 12, 13 and 14.



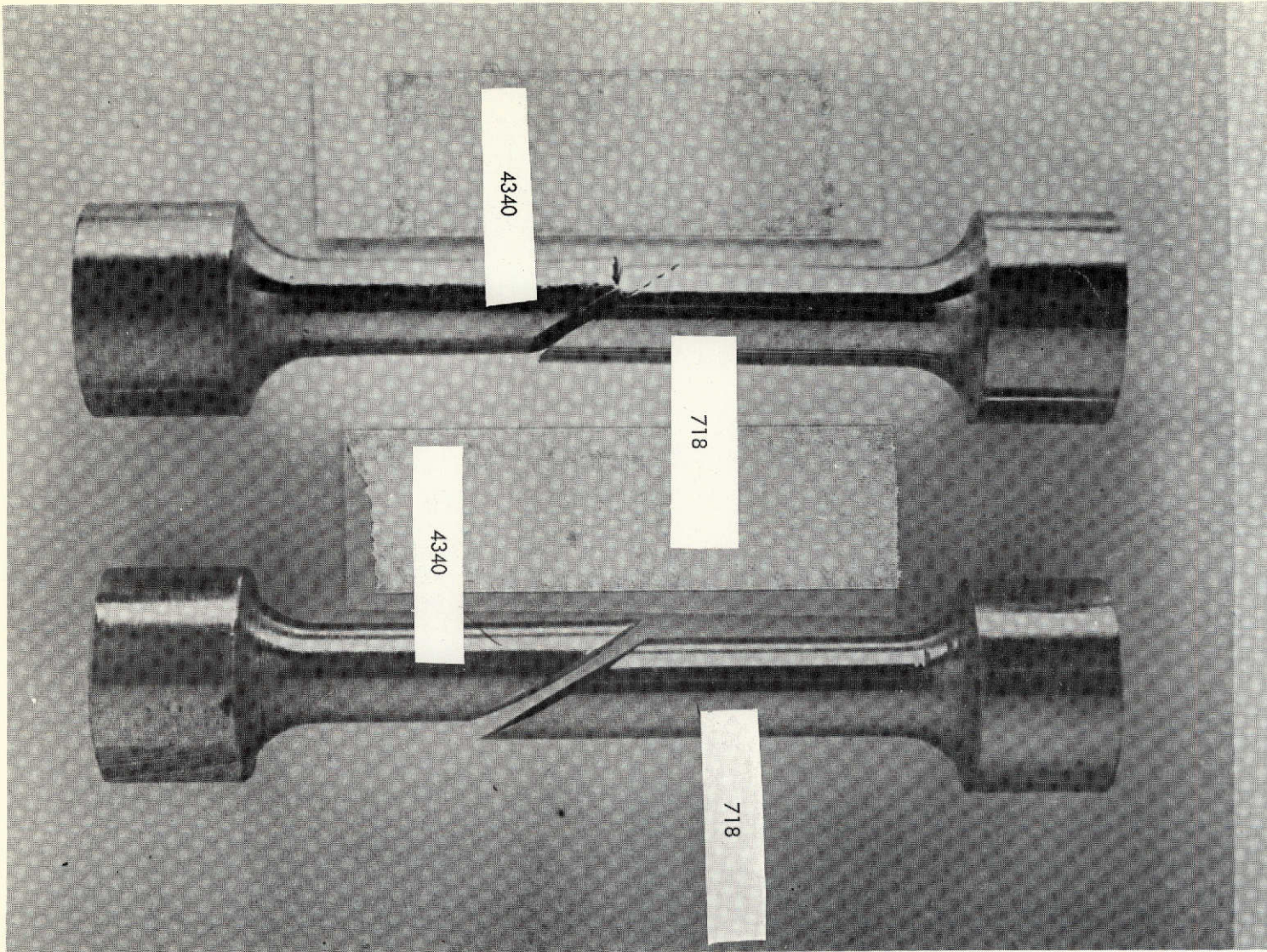


Figure 21. Comparison of Modes of Failure in Tensile Specimens Tested from HIP Welds

Table 4. Tensile Strengths of Welds Prepared with Various Surface Preparations\*

Surface Preparation	Average Ultimate Tensile Strength	
	(psi)	(MN/m <sup>2</sup> )
Cleaned and etched	85,900	582
Cleaned	87,200	601
Gold coated	60,800	419

\* The test data from which this table was prepared are contained in Appendix A, pages 1-8.

high of 79,200 psi ( $546 \text{ MN/m}^2$ ) to a low of 44,700 psi ( $308 \text{ MN/m}^2$ ). No determination of the affect on weld strength of surface preparation on specimens using non-outgassed 4340 components was possible since the results would be masked by the large variations in strength characteristic of non-outgassed material.

The results, besides demonstrating the value of clean pre-weld surfaces, also add further emphasis to the importance of outgassing the steel.

Another form of surface preparation is the machining of surfaces to produce a known level of roughness. This variable's affect on weld quality was studied using the flat-faced specimens described previously. One set of specimens was machined to a 16-32 RMS finish while another set was electric discharge machined to a 250 RMS finish. Both sets were welded using the rotor welding parameters. That this difference in surface finish had no effect on welds produced by the rotor welding process is demonstrated by the identical average bend strength of 128,500 psi ( $886 \text{ MN/m}^2$ ) outer fiber stress associated with each. These data were obtained from Appendix A, pages 13 and 15. At the level of the steel's ductility realized at the  $1730^\circ\text{F}$  ( $944^\circ\text{C}$ ) nominal weld temperatures these degrees of surface roughness are of no consequence in preventing the attachment of intimate contact.

#### D. Weld Temperature

Two temperature levels were investigated in this work, one above [ $1730 \pm 20^\circ\text{F}$  ( $944 \pm 11^\circ\text{C}$ )] and one below [ $1270 \pm 20^\circ\text{F}$  ( $688 \pm 11^\circ\text{C}$ )] the  $A_{e_3}$  temperature. Joint tensile strengths

averaged better than 87,000 psi ( $600 \text{ MN/m}^2$ ) for all high temperature specimens (data from pages 1-3 of Appendix A) while no bonding was achieved at the low temperature. The benefit of the high temperature is that it allows sufficient mobility of contaminants to permit their dispersion from the joint interface. High temperature is not needed to realize intimate contact of components. Sufficient deformation to provide intimate contact (but not welding) was found by visual inspection to occur with the application of 20,000 psi ( $138 \text{ MN/m}^2$ ) hydrostatic pressure for 2 hours (7.2 ks) at only  $1200^\circ\text{F}$  ( $650^\circ\text{C}$ ).

#### E. Weld Hold Time

Based on the two exploratory hold times investigated, the time at which materials to be joined are held at the welding temperature under pressure has no effect on weld strength. This is exemplified by a comparison of parameters and weld strength results from two trials in which hold times of 6.5 hours (23.4 ks) and 4.0 hours (14.4 ks) were used, as given in Table 5.

These data indicate that times less than 4 hours (14.4 ks) are sufficient for the achievement of intimate materials contact and dissolution of any deleterious contaminants. Extending the hold time by 2.5 hours (9.0 ks) offers no advantage over the 4 hours (14.4 ks) used in the rotor welding process.

#### F. Weld Pressure

Bonding pressure was essentially invariant throughout the preliminary treats. This pressure [between 28,300 psi ( $195 \text{ MN/m}^2$ ) and 30,000 psi ( $207 \text{ MN/m}^2$ )] was established by the limit of the autoclave. In this method of solid state welding use of the maximum attainable hydrostatic pressure is desirable in order to provide intimate interface contact in the minimum time and at the minimum temperature.

Table 5. Weld Tensile Strength Data for Two Hold Times\*

Ultimate Tensile Strength			
6.5 Hour Hold Time		4.0 Hour Hold Time	
(psi)	(MN/m <sup>2</sup> )	(psi)	(MN/m <sup>2</sup> )
84,300	581	98,800	681
83,800	578	92,500	637
84,700	585	76,000	524
100,200	691	75,900	523
88,900	613	84,600	584
95,100	656	83,800	578
76,700	529		
Average= 87,700	603	Average=85,300	589

\* The test data from which this table was prepared are contained in Appendix A, pages 1, 2, 3, 5, 6 and 7.



### G. Heat Treatment

Two aspects of heat treatment were incorporated in this program. The first of these was an integral heat treatment to achieve optimum magnetic properties in the 4340 components. This heat treatment was satisfactorily shown to enhance weld strength. However, quantitative comparisons of data on welds made with and without integral heat treatment are not shown here since all the data were obtained on non-outgassed material and thus are both quite variable and unsuited for comparison with welds made by the rotor welding process which utilized outgassing.

In addition, specimens welded using the rotor welding parameters were subjected to post weld heat treatments to ascertain if joint strength would respond to base metal heat treatments. The results of this feasibility study were quite encouraging as shown in Table 6. The data for heat treatments A and C show that for the limited number of heat treatments tried, joint strength could be increased by almost 50 per cent. Higher specimen strength was realized for a joint oriented at  $30^\circ$  (0.523 rad) to the tensile direction rather than normal to this direction. Hence, joint orientation would also have an effect on net section load acceptable for a given design.

It is also worth noting that as seen from the results of the tensile tests the severe thermal shock accompanying oil quenching from temperatures as great as  $1525^\circ\text{F}$  ( $829^\circ\text{C}$ ) had no deleterious effect on weld joint strength.

### H. Magnetic Permeability

The HIP welded rotors, in addition to possessing high weld strength, were also required to have their 4340 pole pieces possess magnetic permeability in excess of 96% of the magnetic permeability of a control sample which was cooled from the austenite range and isothermally held for 8 hours (28.8 Ms) at  $1165^\circ\text{F}$  ( $629^\circ\text{C}$ ). Permeabilities were determined at a magnetizing force of 100 oersteds (7.960 mA/m), this value being the mean of the evaluated range.

Table 6. Effect of Post Weld Heat Treatment and Joint Orientation on Joint Strength

Specimen No.*	Heat Treatment	Hardness, R <sub>C</sub>		Ultimate Tensile Strength of Weld Specimen		Comments
		718	4340	(psi)	(MN/m <sup>2</sup> )	
1	As-Welded	39	12.5	82,500	569	Joint 90° ( $\pi/2$ rad) to load
2	A	32	39	118,000	812	"
3	A	32	39	120,000	826	"
4	B	35	33	110,700	761	"
5	B	35	33	115,000	791	"
6	B	--	--	114,800	789	"
7	C	35	40	120,500	830	"
8	A	--	39	154,000	1062	Parent Metal (4340)
9	A	34		165,500	1141	Parent Metal (718)
10	D	35	42	141,800	975	Joint 30° ( $\pi/6$ rad) to load
11	D	35	42	139,200	960	Joint 30° ( $\pi/6$ rad) to load

\* Material used was from specimens welded in trial X (components cleaned only and welded with rotor welding parameters)

#### Heat Treatments

- A 30 minutes (1.8 ks) at 1525°F (828°C), oil quench, temper 2 hours (7.2 ks) at 950°F (510°C), air cool.
- B 30 minutes (1.8 ks) at 1425°F (773°C), furnace cool to 700°F (372°C), hold for 2 hours (7.2 ks), air cool.
- C 1 hour (3.6 ks) at 1750°F (954°C), air cool to room temperature, heat at 1425°F (773°C) for 6 hours (21.6 ks), oil quench, temper 4 hours (14.2 ks) at 800°F (428°C), air cool.
- D 6 hours (21.6 ks) at 1425°F (773°C), oil quench, temper 4 hours (14.2 ks) at 800°F (428°C), air cool.

Several typical magnetization curves are shown in Figure 23. It was established during this study that the inverse correlation between hardness and magnetic permeability permitted the use of 21 Rockwell C hardness as the maximum hardness to be associated with acceptable permeability. The effect of integral heat treatment on magnetic permeability (as measured by 4340 hardness) is shown by the data of Table 7.

The hardness of specimens included in the rotor welding runs (Y and Z) was Rc 13. The rotor pole pieces thus are expected to possess magnetic permeability in excess of 96% of the control sample.

#### J. Alternate Magnetic Materials

A brief investigation into the welding of Hiperc 50 (50Fe-50Co) to Inconel 718 was undertaken. Type I weld specimens (in which Hiperc 50 was substituted for 4340 steel in the end portion) were welded using the rotor welding process. Joint tensile strengths for these welds are given in Table 8. In all cases failures occurred either entirely through the Hiperc 50 or were initiated there because of the low strength of the Hiperc 50. This material normally has a tensile strength of about 60,000 psi ( $414 \text{ MN/m}^2$ ) when annealed at  $1470^\circ\text{F}$  ( $798^\circ\text{C}$ ) to attain maximum magnetic properties. The scope of this program precluded both this heat treatment being incorporated into the welding cycle and a separate study being conducted to determine possible post-weld thermal treatments.

It is noted from these data that weld joint strength was enhanced by etching the Hiperc 50.

Photomicrographs taken at the interfaces of specimens representing the two surface preparations are presented in Figures 24 and 25. No difference in interface appearance associated with method of surface preparation is noted.



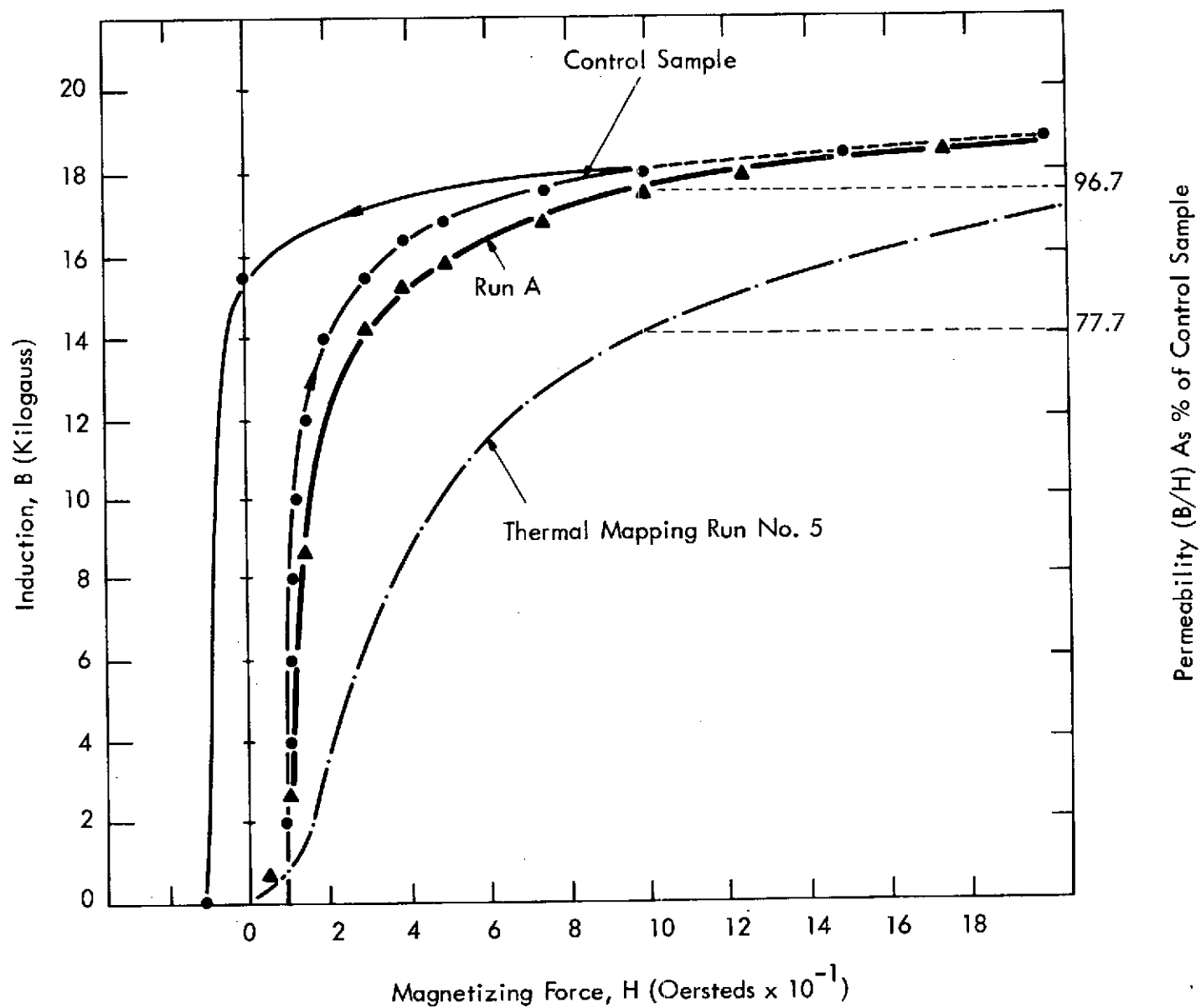


Figure 22. Magnetization Curves for Material From Two Welding Trials Compared to that for a Control Sample

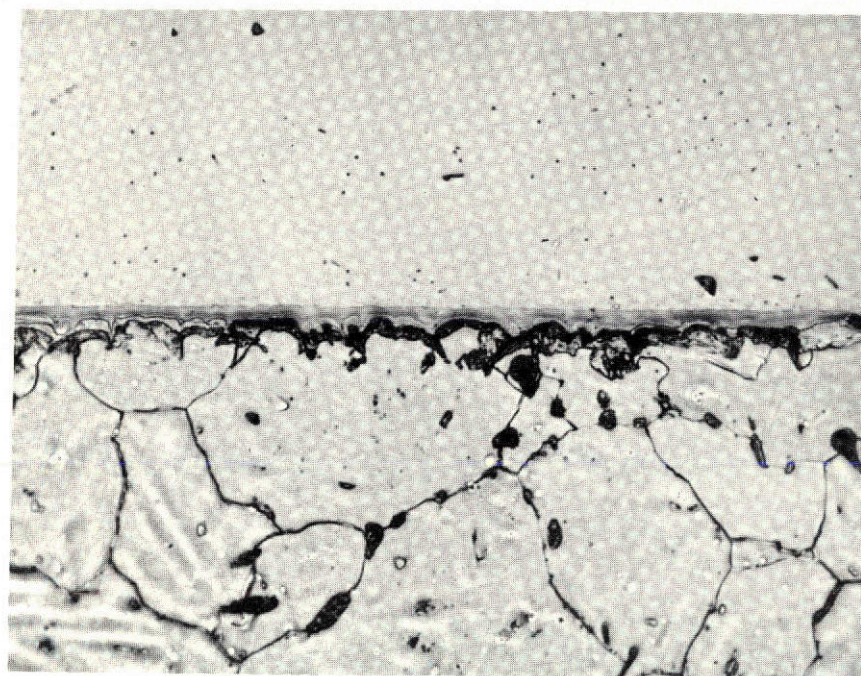
Table 7. Magnetic Permeability of 4340 Steel Associated with a Number of Integral Heat Treatments

Welding Trial No.	Isothermal Heat Treatment Conditions Following Welding in Austenite Range	Magnetic Permeability as % of Control Sample	R <sub>c</sub> Hardness
Control Sample	8 hrs. at 1165°F (28.4 ks at 680°C)	100	20
5*	None	77.7	34
A	10 hrs. at 1100°F (36.0 ks at 594°C)	96.7	21
O	12 hrs. at 1200°F (43.2 ks at 650°C)	---	11
X	12 hrs. at 1200°F (43.2 ks at 650°C)	---	14
Y	12 hrs. at 1200°F (43.2 ks at 650°C)	---	13
Z	12 hrs. at 1200°F (43.2 ks at 650°C)	---	13

\* Preliminary trial (made for the purpose of checking the performance of the autoclave furnace) in which several ring specimens were included.

Table 8. Tensile Strengths of Hiperco 50 - Inconel 718 Welded Couples

Specimen No.	Surface Preparation	Stress at Prop. Limit		Ultimate Tensile Strength (psi)	
		(psi)	(MN/m <sup>2</sup> )	(psi)	(MN/m <sup>2</sup> )
X-1-CH-9	cleaned and etched	32,000	221	48,800	337
X-1-CH-6	cleaned and etched	36,300	250	54,700	377
X-1-MH-9	cleaned only	26,200	181	44,200	305
X-1-MH-6	cleaned only	27,700	191	44,600	308

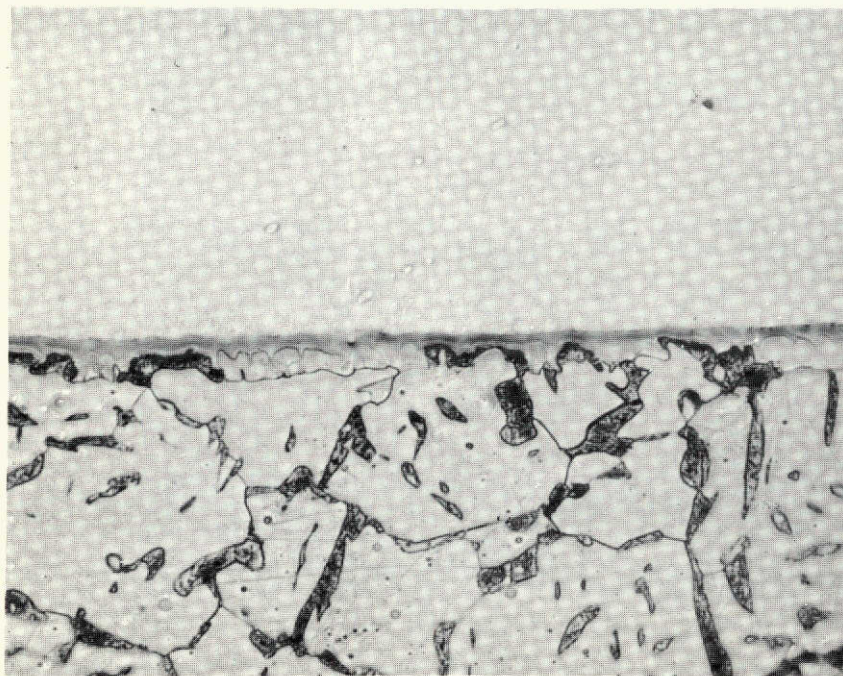


718

Hyperco 50

400X

Figure 23. Microstructure of Inconel 718 - Hyperco 50 Weld Specimen.  
Hyperco 50 was Etched Prior to Welding.



718

Hyperco 50

400X

Figure 24. Microstructure of Inconel 718 - Hyperco 50 Weld Specimen.  
Hyperco 50 was not Etched Prior to Welding.

## V. CONCLUSIONS

1. Fabrication of hardware (such as the rotors in this program) is an ideal application for HIP welding.
2. Hot isostatic pressing not only provides the conditions required to achieve a solid state weld, but inherently provides accommodation of mismatch in joint fit-up which can be anticipated in complex shapes. This is achieved by gross plastic flow which naturally occurs in the presence of a stress high enough to achieve microscopic intimacy of joint surfaces.
3. HIP welding cycles can incorporate integral heat treat cycles. This provides an added advantage of maintaining compressive isostatic pressure to assist in plastic accommodation of thermal strains associated with heat treatment transformations.
4. Degassing of 4340 steel proved to be essential in achieving consistent weld strength.
5. Surface scrubbing and scrubbing followed by etching were equivalent in their relation to weld strength.
6. Welding in excess of the  $Ae_3$  temperature is required to produce high joint strength. This requirement is associated with dispersion of joint interface contaminants. Intimate contact is achieved at a much lower temperature.
7. Heat treatments after bonding can be successfully applied to HIP welded 4340-718 joints to increase their strength.
8. The HIP welding procedure developed during this program produced high magnetic permeability in the 4340 pole pieces.
9. This procedure was shown to be applicable also to the welding of Inconel 718 to Hiperco-50.

## VI. REFERENCES

1. T. J. Moore and K. H. Holko, "Solid State Welding of TD-Nickel Bar", The Welding Journal Research Supplement, Vol. 49 (9), September, 1970.
2. Air Research Drawing No. 699721, Air Research Manufacturing Co., Phoenix, Arizona
3. Air Research Drawing No. 699700, Air Research Manufacturing Co., Phoenix, Arizona
4. W. D. Ludemann, "A Fundamental Study of the Pressure Welding of Dissimilar Metals Through Oxide Layers", report UCRL-50744, October, 1969.

## APPENDIX A

### DATA SUMMARY SHEETS FOR PRELIMINARY WELDING TRIALS



## Appendix A1

### Data Summary for Type II Bond Specimens from Trial O

#### Pre-Bond Specimen Identification

4340 component  
718 component

4-T-C-O  
7-O-C-O

#### Can Identification

0-11

#### Specimen Preparation

cleaned and etched  
4340 components outgassed

#### Bonding Parameters

Temp. ( $^{\circ}$ F)  
Time (Hrs.)  
Pressure (psi)

1710-1750  
6.5  
28,600

#### Parameters for in situ Post-Bond Hold

Temp ( $^{\circ}$ F)  
Time (Hrs.)  
Pressure (psi)

1200  
12  
28,600

#### Interface Condition

Good bond entire length  
of interface. Area  
shown is at region of  
sharpest change in inter-  
face contour.



718

4340

400X

#### Test Results (Tensile)

Proportional Limit (psi)

43,100 (specimen 0-11-C-4, top)

Ultimate Tensile Strength (psi)

45,000 (specimen 0-11-C-2, top)

95,100 (specimen 0-11-C-4, top)

76,700 (specimen 0-11-C-2, top)

## Appendix A2

### Data Summary for Type II Bond Specimens from Trial O

#### Pre-Bond Specimen Identification

4340 component  
718 component

4-S-M-O  
7-O-M-O

#### Can Identification

0-11

#### Specimen Preparation

cleaned only  
4340 components outgassed

#### Bonding Parameters

Temp. ( $^{\circ}$ F)  
Time (Hrs.)  
Pressure (psi)

1710-1750  
6.5  
28,600

#### In-situ Post-Bond Treatment Parameters

Temp. ( $^{\circ}$ F)  
Time (Hrs.)  
Pressure (psi)

1200  
12  
28,600

#### Interface Condition

Good bond entire  
length of interface.



400X

#### Test results (Tensile)

Proportional Limit (psi)  
Ultimate Strength (psi)

44,300 (specimen 0-11-M-4, bottom)  
43,500 (specimen 0-11-M-2, bottom)  
100,200 (specimen 0-11-M-4, bottom)  
88,900 (specimen 0-11-M-2, bottom)

### Appendix A3

#### Data Summary for Type I Bond Specimens from Trial O

##### Pre-Bond Specimen Identification

4340 component  
718 component

4-O-M-O  
7-O-M-O

##### Can Identification

O-1-M

##### Specimen Preparation

cleaned only; 4340 components  
outgassed

##### Bonding Parameters

Temp. ( $^{\circ}$ F)  
Time (Hrs.)  
Pressure (psi)

1710-1750  
6.5  
28,600

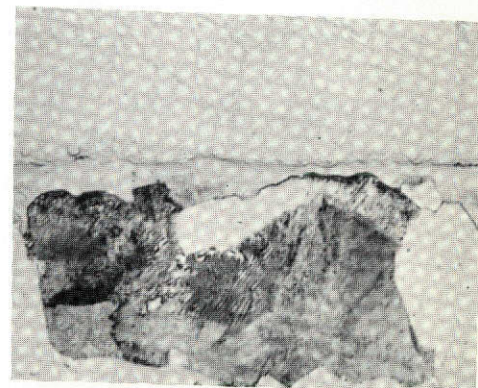
##### In-situ Post-Bond Treatment Parameters

Temp. ( $^{\circ}$ F)  
Time (Hrs.)  
Pressure (psi)

1200  
12  
28,600

##### Interface Condition

Good bond entire  
length of interface.



400X

##### Test Results (Tensile)

Proportional Limit (psi)

42,700 (specimen 0-1-M-9)  
47,300 (specimen 0-1-M-9)

Ultimate Strength (psi)

47,600 (specimen 0-1-M-6)  
84,300 (specimen 0-1-M-9)  
83,800 (specimen 0-1-M-9)  
84,700 (specimen 0-1-M-6)



## Appendix A4

### Data Summary for Type I Bond Specimens from Trial O

#### Pre-Bond Specimen Identification

4340 component  
718 component

4-O-G-O  
7-O-G-O

#### Can Identification

0-1-G

#### Specimen Preparation

gold sputter coated; 4340  
components outgassed

#### Bonding Parameters

Temp. ( $^{\circ}$ F)  
Time (Hrs.)  
Pressure (psi)

1710-1750  
6.5  
28,600

#### In-situ Post-Bond Treatment Parameters

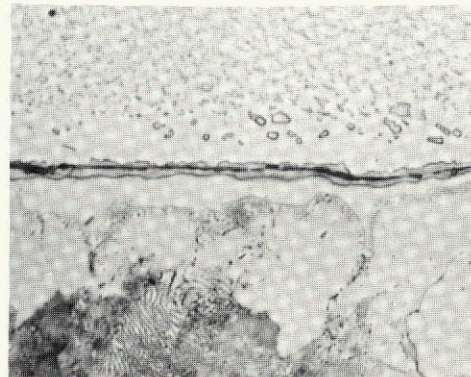
Temp. ( $^{\circ}$ F)  
Time (Hrs.)  
Pressure (psi)

1200  
12  
28,600



#### Interface Condition

4 to 5% of interface  
contains crack through  
the narrower inter-  
diffusion bond.



400X

#### Test Results (Tensile)

Proportional Limit (psi)

45,600 (specimen 0-1-G-9)  
----- (specimen fractured during  
machining)

Ultimate Strength (psi)

44,900 (specimen 0-1-G-9)  
46,900 (specimen 0-1-G-6)  
61,100 (specimen 0-1-G-9)  
----- (specimen fractured during  
machining)  
64,600 (specimen 0-1-G-9)  
54,400 (specimen 0-1-G-6)

## Appendix A5

### Data Summary for Type II Bond Specimens from Trial X

#### Pre-Bond Specimen Identification

4340 component  
718 component

4-S-C-X  
7-O-C-X

#### Can Identification

X-11-C

#### Specimen Preparation

cleaned and etched; 4340  
components outgassed

#### Bonding Parameters

Temp. ( $^{\circ}$ F)  
Time (Hrs.)  
Pressure (psi)

1710-1750  
4  
28,800

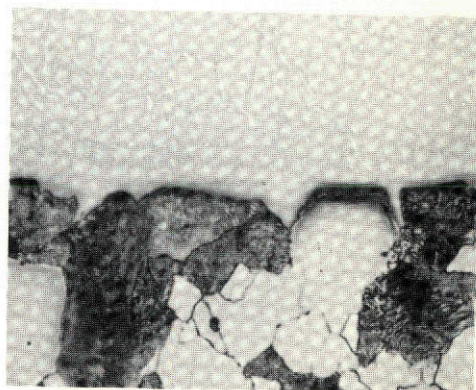
#### In-situ Post-Bond Treatment Parameters

Temp. ( $^{\circ}$ F)  
Time (Hrs.)  
Pressure (psi)

1200  
12  
28,800

#### Interface Condition

Good bond entire  
length of interface.



400X

#### Test Results (Tensile)

Proportional Limit (psi)

50,700 (specimen X-11-C-4, top)

Ultimate Strength (psi)

50,900 (specimen X-11-C-2, top)

98,800 (specimen X-11-C-4, top)

92,500 (specimen X-11-C-2, top)

## Appendix A6

### Data Summary for Type I Bond Specimens from Trial X

#### Pre-Bond Specimen Identification

4340 component  
718 component

4-5-C-X  
7-O-C-X

#### Can Identification

X-1-C

#### Specimen Preparation

cleaned and etched; 4340  
components outgassed

#### Bonding Parameters

Temp. ( $^{\circ}$ F)  
Time (Hrs.)  
Pressure (psi)

1710-1750  
4  
28,800

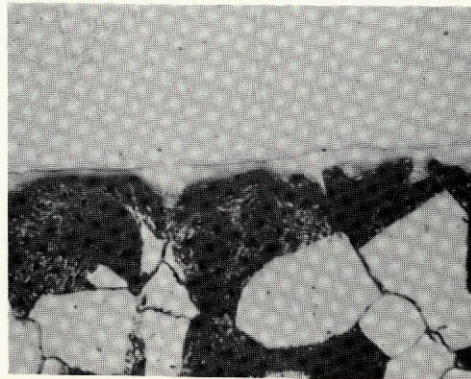
#### In-situ Post-Bond Treatment Parameters

Temp. ( $^{\circ}$ F)  
Time (Hrs.)  
Pressure (psi)

1200  
12  
28,800

#### Interface Condition

Bonded entire length of  
interface but with some  
evidence of narrower  
diffusion bond.



400X

#### Test Results (Tensile)

Proportional Limit (psi)  
Ultimate Strength (psi)

50,900 (specimen X-1-C-9)  
52,200 (specimen X-1-C-6)  
76,000 (specimen X-1-C-9)  
75,900 (specimen X-1-C-6)



## Appendix A7

### Data Summary for Type I Bond Specimens from Trial X

#### Pre-Bond Specimen Identification

4340 component	4-0-M-X
718 component	7-0-M-X

#### Can Identification

X-1-M

#### Specimen Preparation

cleaned only; 4340 components  
outgassed

#### Bonding Parameters

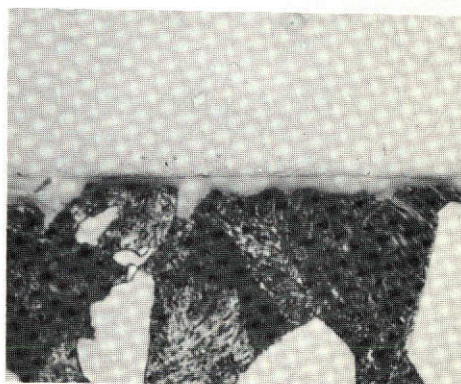
Temp. (°F)	1710-1750
Time (Hrs.)	4
Pressure (psi)	28,800

#### In-situ Post-Bond Treatment Parameters

Temp. (°F)	1200
Time (Hrs.)	12
Pressure (psi)	28,800

#### Interface Condition

Good bond entire length  
of interface.



400X

#### Test Results (Tensile)

Proportional Limit (psi)	43,400 (specimen X-1-M-9)
	50,100 (specimen X-1-M-6)
Ultimate Strength (psi)	84,600 (specimen X-1-M-9)
	83,800 (specimen X-1-M-6)

## Appendix A8

### Data Summary for Type I Bond Specimens from Trial X

#### Pre-Bond Identification

4340 component  
718 component

4-0-G-X

7-0-G-X

#### Can Identification

X-1-G

#### Specimen Preparation

gold sputter coated; 4340  
components outgassed

#### Bonding Parameters

Temp. ( $^{\circ}$ F)  
Time (Hrs.)  
Pressure (psi)

1710-1750

4

28,800

#### In-situ Post-Bond Treatment Parameters

Temp. ( $^{\circ}$ F)  
Time (Hrs.)  
Pressure (psi)

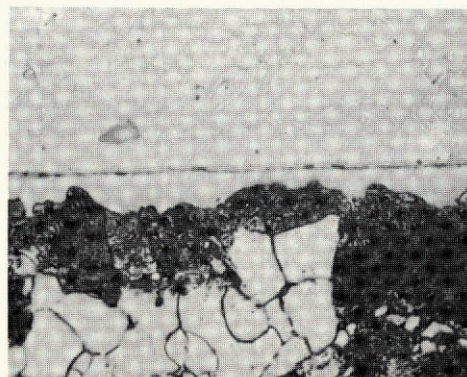
1200

12

28,800

#### Interface Condition

Cracking observed  
throughout much of  
narrower interdiffusion  
bond.



400X

#### Test Results (Tensile)

Proportional Limit (psi)

45,400 (specimen X-1-G-9)

None found (specimen X-1-G-6)

Ultimate Strength (psi)

79,200 (specimen X-1-G-9)

44,700 (specimen X-1-G-6)



## Appendix A9

### Data Summary for Type I Bond Specimens from Trial A

#### Pre-Bond Specimen Identification

4340 component	4-0-C-A
718 component	7-0-C-A

#### Can Identification

A-1-C

#### Specimen Preparation

cleaned and etched

#### Bonding Parameters

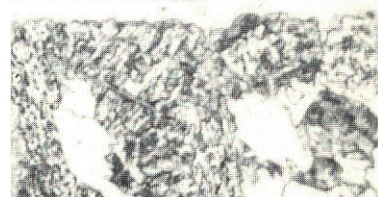
Temp. ( $^{\circ}$ F)	1650-1750
Time (Hrs.)	4
Pressure (psi)	30,000

#### In-situ Post-Bond Treatment Parameters

Temp. ( $^{\circ}$ F)	1100
Time (Hrs.)	10
Pressure (psi)	30,000

#### Interface Condition

Good bond entire  
length of interface.



(400X)

#### Test Results (Tensile)

Proportional Limit (psi)	66,100 (specimen A-1-C-9)
	58,400 (specimen A-1-C-6)
Ultimate Strength (psi)	98,200 (specimen A-1-C-9)
	95,400 (specimen A-1-C-6)

## Appendix A10

### Data Summary for Type I Bond Specimens from Trial A

#### Pre-Bond Specimen Identification

4340 component	4-0-M-A
718 component	7-0-M-A

Can Identification	A-1-M
--------------------	-------

Specimen Preparation	cleaned only
----------------------	--------------

#### Bonding Parameters

Temp. (°F)	1650-1750
Time (Hrs.)	4
Pressure (psi)	30,000

#### In-situ Post-Bond Treatment Parameters

Temp. (°F)	1100
Time (Hrs.)	10
Pressure (psi)	30,000

#### Interface Condition

Good bond entire  
length of interface.

#### Test Results (Tensile)

Proportional Limit (psi)	70,300 (specimen A-1-M-9) None found (specimen A-1-M-6)
Ultimate Strength (psi)	71,840 (specimen A-1-M-9) 72,560 (specimen A-1-M-6)

## Appendix A11

## Data Summary for Type II Bond Specimens from Trial A

## Pre-Bond Specimen Identification

4340 component

718 component

4-0-M-A

7-0-M-A

## Can Identification

A-11

## Specimen Preparation

cleaned only

## Bonding Parameters

Temp. ( $^{\circ}$ F)

1650-1750

Time (Hrs.)

4

Pressure (psi)

30,000

## In-situ Post-Bond Treatment Parameters

Temp. ( $^{\circ}$ F)

1100

Time (Hrs.)

10

Pressure (psi)

30,000

## Test Results (Tensile)

None

Specimens fractured at interface during machining to tensile specimens.

## Appendix A12

### Data Summary for Type II Bond Specimens from Trial X

#### Pre-Bond Specimen Identification

4340 component  
718 component

4-V-C-X  
7-0-C-X

#### Can Identification

X-11-C

#### Specimen Preparation

cleaned and etched; 4340 components  
outgassed; vacuum melted 4340 used.

#### Bonding Parameters

Temp. ( $^{\circ}$ F)  
Time (Hrs.)  
Pressure (psi)

1710-1750  
4  
28,800

#### In-situ Post-Bond Treatment Parameters

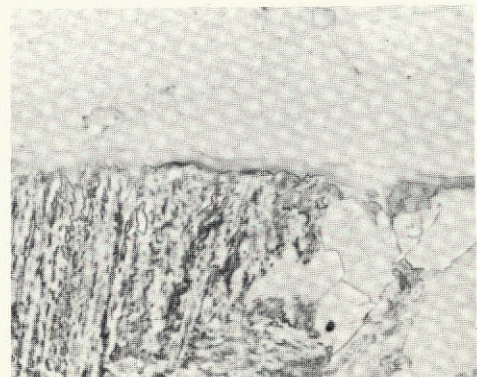
Temp. ( $^{\circ}$ F)  
Time (Hrs.)  
Pressure (psi)

1200  
12  
28,800



#### Interface Condition

Good bond entire  
length of interface.



400X

#### Test Results (Tensile)

Proportional Limit (psi)  
  
Ultimate Strength (psi)

48,800 (specimen X-11-C-4, bottom)  
48,300 (specimen X-11-C-2, bottom)  
101,400 (specimen X-11-C-4, bottom)  
104,300 (specimen X-11-C-2, bottom)

## Appendix A13

### Data Summary for Simple Bond Specimens from Trial Y

#### Pre-Bond Specimen Identification

4340 component  
718 component

4-S-C-Y  
7-0-C-Y

#### Can Identification

Y-S-C

#### Specimen Preparation

cleaned and etched; 4340  
components outgassed

#### Bonding Parameters

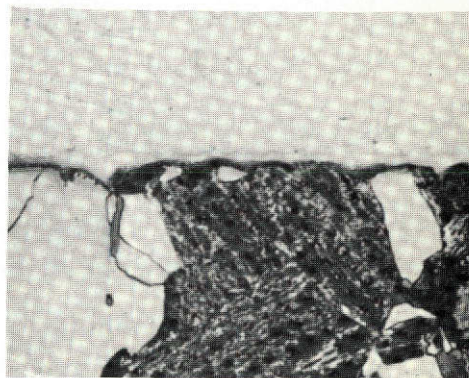
Temp. (°F)	1710-1750
Time (Hrs.)	4
Pressure (psi)	29,000

#### In-situ Post-Bond Treatment Parameters

Temp. (°F)	1200
Time (Hrs.)	12
Pressure (psi)	29,000

#### Interface Condition

Good bond entire  
length of interface.



400X

#### Test Results (Bend)

<u>Specimen No.</u>	<u>Fracture Stress (psi)</u>	<u>% of Fracture Surface Exhibiting Ductility</u>
Y-S-C-1	111,600	95
2	122,800	100
3	122,100	100
4	123,300	100
5	113,200	95
6	140,300	100
7	130,600	100
8	159,000	95
9	134,000	100



## Appendix A14

### Data Summary for Simple Bond Specimens from Trial Z

#### Pre-Bond Specimen Identification

4340 component  
718 component

4-V-C-Z  
7-0-C-Z

#### Can Identification

Z-S-VC

#### Specimen Preparation

cleaned and etched; 4340 components  
outgassed; vacuum melted 4340 used.

#### Bonding Parameters

Temp. (°F)  
Time (Hrs.)  
Pressure (psi)

1710-1750  
4  
29,000

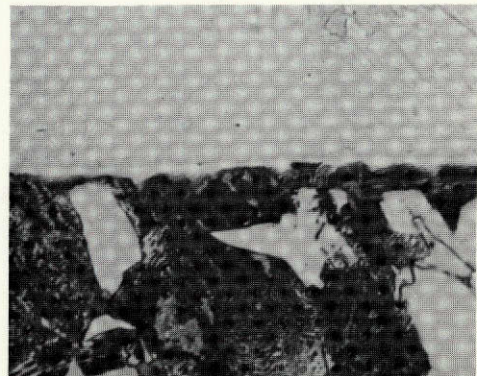
#### In-situ Post-Bond Treatment Parameters

Temp. (°F)  
Time (Hrs.)  
Pressure (psi)

1200  
12  
29,000

#### Interface Condition

Good bond entire  
length of interface.



400X

#### Test Results (Bend)

<u>Specimen No.</u>	<u>Fracture Stress (psi)</u>	<u>% of Fracture Surface Exhibiting Ductility</u>
Z-S-VC-1	118,200	100
2	140,900	75
3	144,900	100
4	135,800	75
5	120,700	30
6	108,400	100
7	107,800	95
8	105,400	100
9	93,900	100

## Appendix A15

### Data Summary for Simple Bond Specimens from Trial Y

#### Pre-Bond Specimen Identification

4340 component

718 component

4-T-RC-Y

7-O-RC-Y

#### Can Identification

Y-S-CR

#### Specimen Preparation

cleaned and etched; 4340 components outgassed and roughened by EDM machining.

#### Bonding Parameters

Temp. ( $^{\circ}$ F)

1710-1750

Time (Hrs.)

4

Pressure (psi)

29,000

#### In-situ Post-Bond Treatment Parameters

Temp. ( $^{\circ}$ F)

1200

Time (Hrs.)

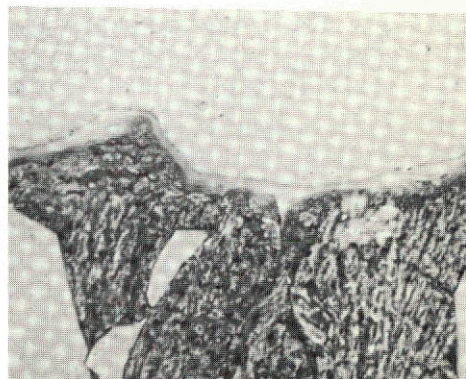
12

Pressure (psi)

29,000

#### Interface Condition

Good bond entire  
length of interface.



400X

#### Test Results (Bend)

<u>Specimen No.</u>	<u>Fracture Stress (psi)</u>	<u>% of Fracture Surface Exhibiting Ductility</u>
Y-S-CR-1	163,500	100
2	111,200	95
3	124,300	95
4	116,000	100
5	130,000	95
6	97,100	100
7	129,800	90
8	147,700	100
9	138,500	95

## Appendix A16

### Data Summary for Simple Bond Specimens from Trial O

#### Pre-Bond Specimen Identification

4340 component  
718 component

4-S-M-0  
7-0-C-0

#### Can Identification

0-11

#### Specimen Preparation

Inconel 718 cleaned and etched;  
4340 cleaned and outgassed.

#### Bonding Parameters

Temp. (°F)  
Time (Hrs.)  
Pressure (psi)

1710-1750  
6.5  
28,600

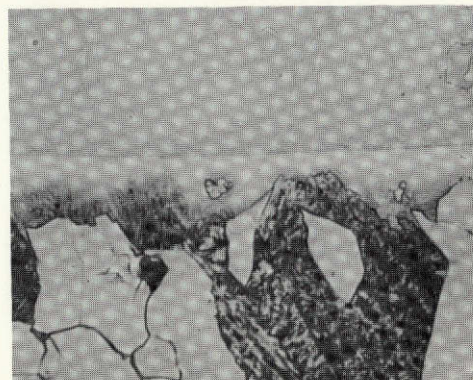
#### In-situ Post-Bond Treatment Parameters

Temp. (°F)  
Time (Hrs.)  
Pressure (psi)

1200  
12  
28,600

#### Interface Condition

Slight crack for 20%  
of interface; remainder  
of interface looks very  
good as shown here.



400X

#### Test Results (Bend) \*

<u>Specimen No.</u>	<u>Fracture Stress (psi)</u>
O-S- $\frac{C}{M}$ -1	120,400
2	135,980
3	128,050
4	121,700
5	154,380
6	103,910
7	109,390
8	103,050

\* The bend test coupons were created  
by removing sections from the mid-  
length of Type II specimens.



## Appendix A17

### Data Summary for Type I Bond Specimens from Trial A

#### Pre-Bond Specimen Identification

4340 component	4-0-G-A
718 component	7-0-G-A

#### Can Identification

A-1-G

#### Specimen Preparation

gold sputter coated

#### Bonding Parameters

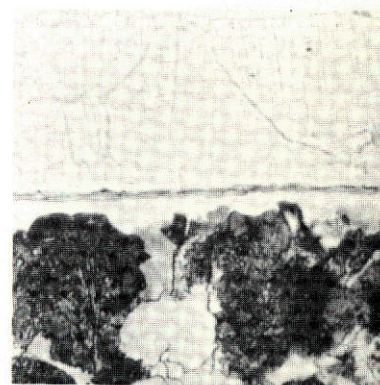
Temp. (°F)	1650-1750
Time (Hrs.)	4
Pressure (psi)	30,000

#### In-situ Post-Bond Treatment Parameters

Temp. (°F)	1100
Time (hrs.)	10
Pressure (psi)	30,000

#### Interface Condition

Thin crack noted to occur through narrower interdiffusion zone for portion of bond interface.



400X

#### Test Results (Tensile)

Proportional Limit (psi)	70,160 (specimen A-1-G-9)
	None found (specimen A-1-G-6)
Ultimate Strength (psi)	76,480 (specimen A-1-G-9)
	58,240 (specimen A-1-G-6)

## Appendix 18

### Data Summary for Type II Bond Specimens from Trial A

#### Pre-Bond Specimen Identification

4340 component	4-0-N-A
718 component	7-0-G-A

Can Identification	A-1-+
--------------------	-------

Specimen Preparation	Inconel 718 gold sputter coated; 4340 steel nickel sputter coated
----------------------	--

#### Bonding Parameters

Temp. (°F)	1650-1750
Time (Hrs.)	4
Pressure (psi)	30,000

#### In-situ Post-Bond Treatment Parameters

Temp. (°F)	1100
Time (Hrs.)	10
Pressure (psi)	30,000

#### Interface Condition

Interface sound for  
entire length of specimen.

#### Test Results (Tensile)

Proportional Limit (psi)	None found (specimen A-1-+-9) None found (specimen A-1-+-6)
Ultimate Strength (psi)	61,920 (specimen A-1-+-9) 53,360 (specimen A-1-+-6)

## Appendix A19

### Data Summary for Type II Bond Specimens from Trial A

#### Pre-Bond Specimen Identification

4340 component	4-0-N-A
718 component	7-0-G-A

#### Can Identification

A-11

#### Specimen Preparation

Inconel 718 gold sputter coated;  
4340 steel nickel sputter coated.

#### Bonding Parameters

Temp. ( $^{\circ}$ F)	1650-1750
Time (Hrs.)	4
Pressure (psi)	30,000

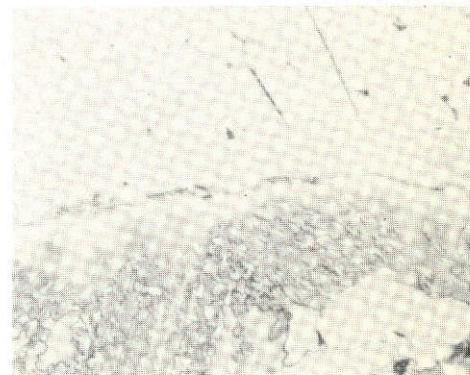
#### In-situ Post-Bond Treatment Parameters

Temp. ( $^{\circ}$ F)	1100
Time (Hrs.)	110
Pressure (psi)	30,000



#### Interface Condition

Portion of interface  
which contained  
porosity.



400X

#### Test Results

Proportional Limit (psi)	69,120 (specimen A-11--2, bottom)
	None found (specimen A-11--4, bottom)
Ultimate Strength (psi)	78,880 (specimen A-11--2, bottom)
	18,400 (specimen A-11--4, bottom)